# Chapter 2

## FA-L-proline catalyzed Asymmetric Direct Aldol reaction in Aqueous system :

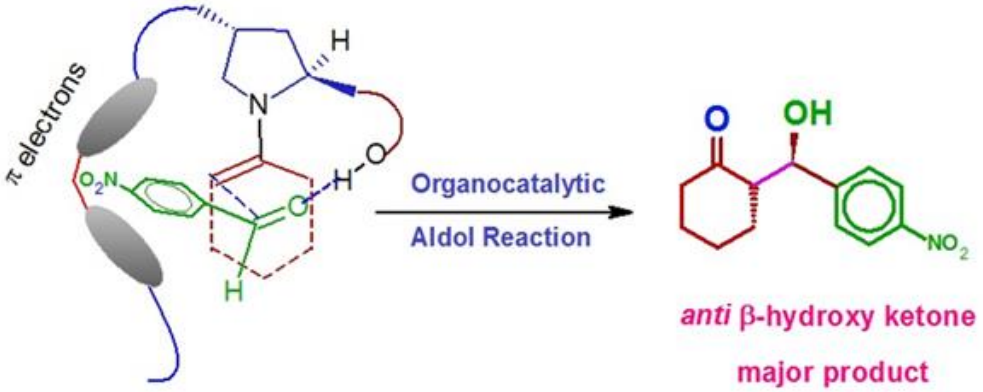


## Molecular Conformations Affect Chiral Induction

## 2.1 Introduction

Aldol reaction is one of the most sought reactions in the field of asymmetric synthesis due to its wide applications ranging from total synthesis of enantiomerically pure natural products to biologically active molecules.[1-5] Work in the field got its first recognition in 1971 when proline was reported as an organocatalyst for intramolecular Aldol transformation (Hajos-Parris-Eder-Sauer-Wiechert reaction)[6-8] and followed by a report on intermolecular Aldol reaction.[9] These milestone steps in the field allowed to induct chirality in Aldol products, β-hydroxy aldehydes or ketones, using proline like amino acids as small molecular organocatalyst. It is noteworthy that chiral auxiliaries like S-BINOL and other substituted enantio-pure diols are not required for the purpose. Moreover, it favors only one cross-Aldol product over self-condensation without using any specific enol equivalents like silylenol ethers (Mukaiyama Aldol reactions) or lithium enolates.[10, 11] This kind of direct cross Aldol reaction is made possible due to the proximity of secondary amine and carboxylic groups in the proline moiety. The reaction is initiated by the covalent interaction of nitrogen atom of secondary amine with nucleophile (donor) resulting in the formation of enamine, thereby activating the donor component.[12, 13] This is quite the same action carried out by trimethylsilyl chloride (SiMe3Cl) or lithium diisopropyl amine (i-Pr2.N.Li) in forming the enol equivalent in a routine protocol.[14] In a similar manner, carboxylic acid functionality of proline activates the Aldol acceptor through H-bonding proton transfer. These electronic interactions stabilize transition state and steric interactions among the donor-acceptor and catalyst make preferentially attack one of the two diastereotopic faces.[15] Above studies established that stereoselective direct Aldol reaction can be carried out by controlling the electronic and steric factors in the catalytic proline moiety. Many efforts have been made to achieve the purpose. Sutar et al. synthesized a series of pyrrolidine derivatives. They adopted variations in the proline structure by altering the steric at the α-position, the position of the carbonyl group, and the acidities of the H-bonding sites. It had been observed that additional steric at the α-position of proline was detrimental for catalytic activity and enantioselectivity. Further, the position of the carbonyl group in the pyrrolidine derived amides is important and, easily accessible prolinamides were found much better than hindered ones.[16] Vishnumaya et al designed L-proline based chiral organocatalyst having a gem-diphenyl group. It has been claimed that pKa value of hydroxyl group involved in the H-bonding with the acceptor aldehyde can be increased by gem-diphenyl group, resulting in a structurally compact transition state responsible for high enantioselectivity and reactivity.[17]

With the development in the field, it has been realized that (i) unmodified proline, being highly polar and insoluble in non-polar solvents, the proline mediated reaction is carried out in an excess of one of

the Aldol substrate (usually donor) as the solvent,[18, 19] (ii) if the reaction is carried out in water, considering 'green aspects',[20] the enantiomeric induction is hampered and the unsubstituted proline does not catalyse Aldol reaction in water [21] and (iii) large amount of catalyst loading is required for a single cycle of reaction. Also, different terminologies were coined when water was involved in an Aldol reaction like, 'in water', 'on water', 'in presence of water' etc.[22] Hayashi proposed that a reaction 'in water' can be considered when all the participating reactants dissolve homogeneously in water (or buffer, for pH control). The terminology '*reaction in presence of water*' can be used for a reaction that proceeds in a concentrated organic phase with water being present as a second phase that influences the reaction in the organic phase. [23] However, reports on Aldol catalysis 'in water' are rare and is a challenge to the filed to carry out organic transformations in aqueous media with a high enantiomeric induction. It has been pointed out that Aldol catalysis '*in presence of water*' can be carried out by using emulsification (generally water in oil, w/o) technique. This can be achieved either by mixing long chain fatty acid with proline derivative [24] or, by introducing amphiphilic property in the proline moiety itself. Based on these strategies, Hayashi et al developed various derivatives of 4-hydroxyproline (1, Scheme 2). They observed formation of emulsion in the reaction mixture and neither very long nor very short chains were effective for the purpose. The catalyst with n = 12 was found to be the most efficient in terms of diastereo- and enantioselectivities for Aldol reaction between o-chlorobenzaldehyde and propanone (5 equiv.) in presence of 18 eqiv. of water for 24 h. They were able to achieve 39-62 % yield with 20:1 anti/syn and 99 %ee for 10 mole% catalyst loading.[25] Zhang et al substituted the hydroxyl group of 4-hydroxyprolinamide with phenoxy. They introduced variation in the amide aromatic ring with different bulky alkyl groups. They proposed that the phenoxy group at the 4-position of prolinamide moiety can stabilize the transition state of Aldol reaction between aldehyde and cyclohexanone by providing extra H-bonding with aldehyde through water. These changes result in high diastereo- and enantioselectivity in aqueous media.[26] Further, Zhong et al synthesized three ester derivatives of 4-hydroxyproline (n = 10, 12 and 18 of 1) having long hydrocarbon chain at the 4- position and prepared their o/w and w/o emulsions. They obtained metastable, unstable or, no emulsion at all, using chiral catalysts. The reported emulsion systems were tested for Aldol reaction between cyclohexanone and 4-nitrobenzaldehyde and, more than 95% yield with 99 %ee and 92-94 %dr were achieved in 13-24 h.[27] Use of w/o emulsion is not recommendable for the purpose due to lower content of water which ruin the greenness of the process.

These accounts suggest that stereo induction can be carried out in the Aldol product by inserting either H-bonding or steric 'element' at the 2-position of the pyrrolidine ring of proline catalyst. In the present

study, we have demonstrated that stereo induction in the Aldol product can be achieved by controlling sterics and electronics at remote site (Forth position) of the pyrrolidine ring. For the purpose, we have synthesized esters of long chain oleic, linoleic and lenolenic acids with *trans*-4-hydroxy-L-proline. Model Aldol reaction between cyclohexanone and p-nitrobenzaldehyde has been carried out using o/w and w/o emulsions (formed by the synthesized catalysts) by changing oil (cyclohexanone) to water ratio in the reaction mixture. Performance based designing of the molecular framework of the catalyst leads to favour the single stereoisomer as major product of the Aldol reaction. Efficiency- emulsion stability relationship has been proposed for the Aldol transformation. Reasons and the mechanism for favouring a given stereoisomer having two chiral centres as major product has been proposed and corroborated by computational analysis.

## 2.2 Experimental

Synthesis of derivatives of trans-4-hydrdroxy-L-proline has been designed with a logic: (i) the hydrophilic-lipophilic balance of the proline catalyst, having the long chain alkyl tail at the 4- position, would affect the stability of emulsion and in turn the selectivity of the Aldol product; (ii) the emulsion can be stabilized by inserting stabilizing element in the lipophilic tail (one of the ways, to achieve this object, is by the introduction of π- bond in the centre of hydrocarbon chain, Fig.1); (iii) due to emulsifying effect, stable droplet formation of aqueous or non-aqueous media into other could be resulted (the emulsion droplet becomes more compact/discrete) via π-π interactions among hydrocarbon tails (Fig. 2); (iv) the cis-olefinic bond in the hydrocarbon chain can induce rigidity in the movement and help to attain stable conformation depending on the polarity of the droplet forming media and (v) molecular conformations can be controlled on increasing the number of π bonds in the chain.

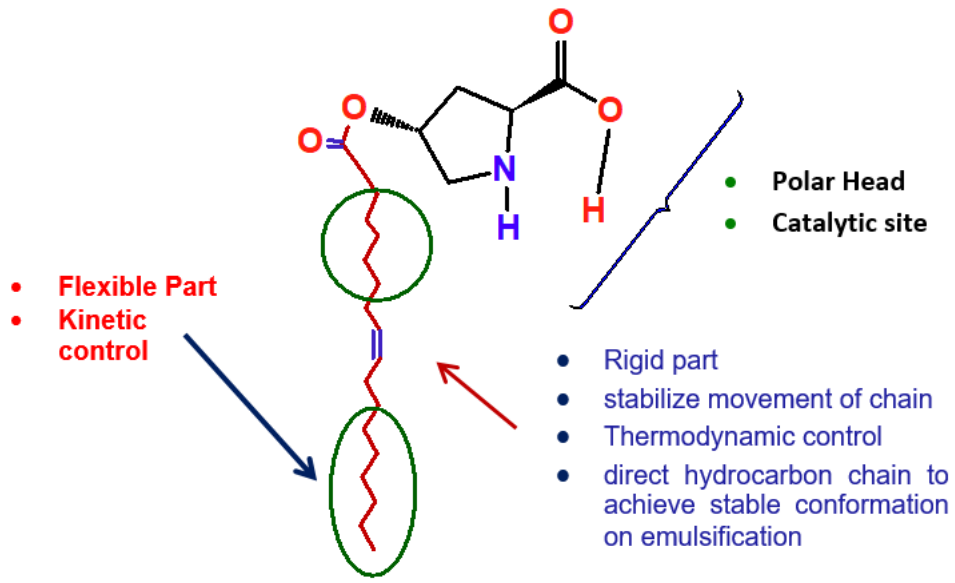


**Fig. 1.** Strategies to control hydrophilic-lipophilic balance and molecular conformation in proline based organocatalyst.

On the basis of these arguments, we synthesized four amphiphilic molecules by *O*-acylation of *trans*-4-hydroxy-L-proline (derived from cheap collagen protein) [19] with fatty acids (derived from the cheap and easily available castor oil) (**2-5**; Scheme 1 and 2).

**Materials**

Stearic acid, oleic acid, trans-4-hydrxy-L-proline and 4-nitrobenzaldehyde were purchased from Loba chemie Pvt. Ltd., India. Linoleic acid and linolenic acid were purchased from TCI Chemicals (India) Pvt. Ltd., oxalyl chloride and acetone from Spectrochem India, cyclohexanone from SRL, India, trifluroacetic acid, diethyl ether, ethyl acetate and petroleum ether 60-80 from S.D. Fine Chemical Ltd., India. All solvents, other than above were purchased from Spectrochem Pvt. Ltd., India. All chemicals were used without further purification.

***O*-acylation of trans-4-hydroxy-L-proline**

For the synthesis of compounds **3**, **4** and **5**, 6 mL of oxalyl chloride (0.07 mole) was slowly added in a fatty acid (4 g, 0.014 mole) at 0-5 $^{o}$C in 2-3 h `under stirring. The yellow coloured liquid formed was kept under vacuum for 3 h to remove unreacted oxalyl chloride and trapped gases. In a separate RBF, 0.92 g of *trans*-4-hydroxy-L-proline (0.007 mole) was slowly added in 6 mL trifluroacetic acid at 0-5 $^{o}$C and stirred until clear solution was obtained. Then, the acid chloride synthesized above was slowly

added to this mixture. The mixture was kept under stirring for 6 h. The product was separated and purified through column chromatography by using ethyl acetate and methanol (1:1) as mobile phase. Compound **2** was synthesized by dissolving 4g (0.014 mole) of stearic acid in 6 mL dichloromethane, remaining procedure was similar as above.

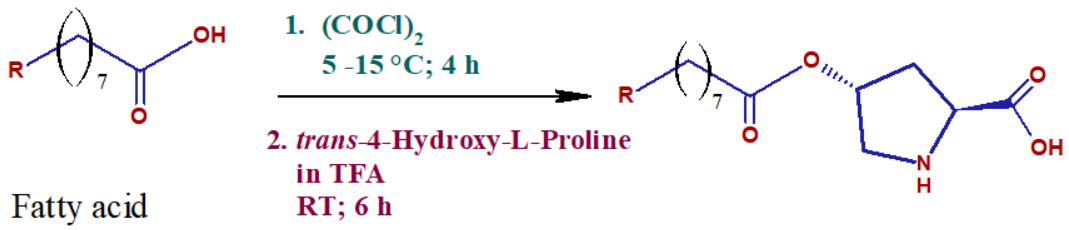


Fatty acid

Where R=

$CH_3(CH_2)_9$-

$CH_3(CH_2)_7CH{=}CH$-

$CH_3(CH_2)_4CH{=}CH\ CH_2CH{=}CH$-

$CH_3CH_2CH{=}CHCH_2CH{=}CHCH_2CH{=}CH$-

**Scheme 1.** *O*-Acylation of *trans*-4-Hydroxy-L-proline with saturated and unsaturated fatty acids (FA).

**Emulsion stability test**

For w/o type, 4 mg (0.01 mmole) of catalyst (**3-5**) was mixed in 2 mL cyclohexanone and the mixture was stirred. On clear solution, 1 mL of water was added and the mixture was stirred vigorously for 2 min. The DLS study and optical microscopy was performed on these systems. For o/w type, 4 mL water was added and similar procedure was performed (2.6.3, chart 1).

**Synthesis of (*R*)-2-((*S*)-hydroxy (4-nitrophenyl) methyl) cyclohexan-1-one (The model Aldol reaction)**

Compound (*2S,4R*)-4-(oleyloxy)pyrrolidine-2-carboxylic acid (**2, 3, 4** or **5**) (13 mg, 0.032 mmol), was added to a mixture of 4-nitrobenzaldehyde (50 mg, 0.33 mmol) and cyclohexanone (250 µL, 2.68 mmol) in water (500 µL) for o/w emulsion at RT and the mixture was stirred for 10 to 24 h. Then, the

mixture was extracted with ethyl acetate and the combined organic extracts were dried over anhydrous $Na_2SO_4$, and concentrated by applying vacuum after filtration. Purification on column chromatography (petroleum ether/ethyl acetate=0.8/0.2) gave (R)-2-((S)-hydroxy (4-nitrophenyl) methyl) cyclohexan-1-one, having >99% ee (by HPLC) on a Chiralpak AD-H column, λ = 210 nm, iPrOH/hexane, 20:80, 0.7 mLmin-1; $t_R$ = 17.8 min (major), 14.2 min (minor). The % dr (*anti: syn*= 80:20) calculated from $^1$H NMR.

### 2.3 Results and Discussion

The synthesized compounds were well characterized by using spectroscopic techniques (See Supporting Information). Being amphiphilic in nature, the synthesized catalyst forms both o/w and w/o emulsions on addition of a specific amounts of cyclohexanone and water with constant stirring. Optical microscopic images and Dynamic Light Scattering (DLS) phenomenon are the direct evidences for the formation and stability of the emulsion (SI 2.6.1 and 2.6.2).

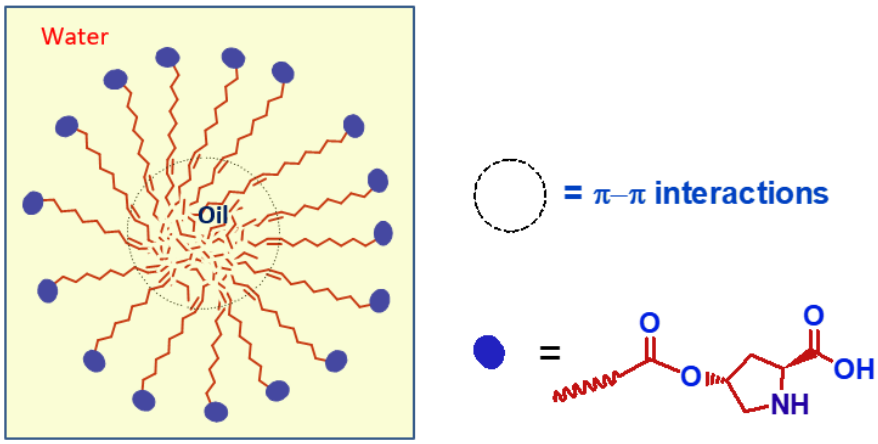


**Fig. 2.** Proposed π - π interactions among hydrocarbon chains in droplet core during o/w emulsification by catalytic molecules **2-5**.

Catalyst **2** could not form a stable suspension due to its structure enforced solubility issue. On introduction of the olefinic bond to the 9-10 position of $C_{18}$ chain of **2**, due to disruption in the close packing present previously, results in a viscous yellowish fluid. The colour and viscosity become more intense on increasing the number of 'lonely' olefinic bonds (separated by sp3 carbon) in the hydrocarbon chain, also supported from UV-visible spectra (SI 19). Fluidic compounds (**3 -5**) were able to form fairly stable o/w and w/o emulsions. The emulsions then become metastable to unstable with time as can be seen in the microscopic images (SI 1).[28] DLS results also support these observations (SI 2). The emulsion stability studies were carried out for o/w and w/o systems with all

**2-5** catalysts in fixed amount of cyclohexanone-water mixture (SI 3). It can be observed from SI 3 that o/w emulsion formed by **4** and **5** are highly stable at RT while, **3** formed unstable emulsion and **2** formed white metastable suspension. Therefore, stable o/w systems were selected for Aldol reaction.

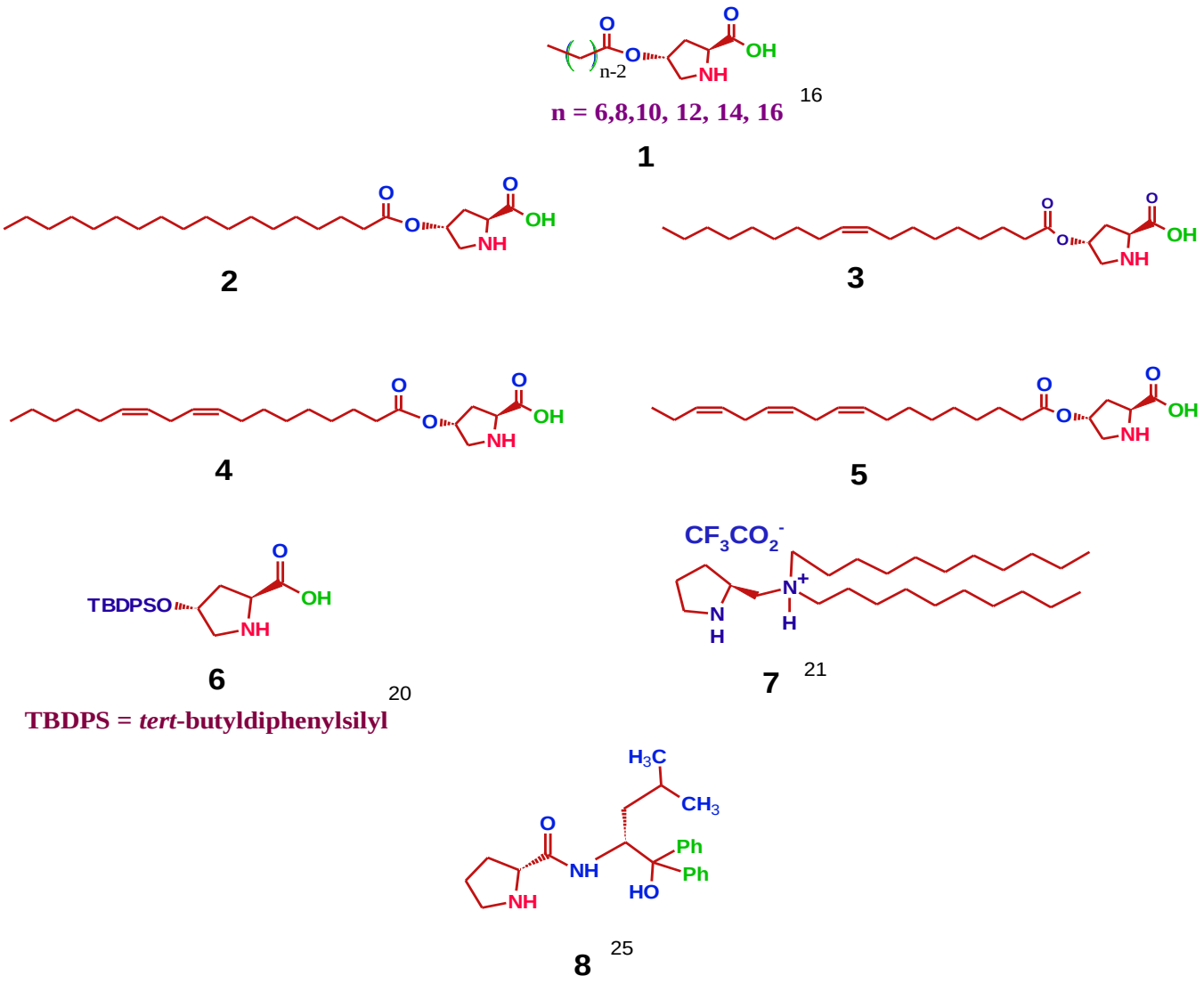


**Scheme 2.** Proline based organocatalysts discussed in this study. Compounds **2-5** reported in this work, the references for the remaining catalysts given in the text.

The model Aldol reaction between 4-nitrobenzaldehyde (**10**) and cyclohexanone (**9**) was carried out in o/w emulsion formed with 10% loaded **2-5** catalysts (Table 1). It can be observed from Table 1 that **2**, even though form unstable suspension, has good conversion ability. It produced 90% yield with 81 %dr and 96 %ee in 24 h. It is interesting to note that **3** with single π bond showed excellent conversion ability but poor %dr. It showed 99% conversion ability with 50 %dr and 95 %ee within 24 h.

**Table 1.** Aldol reaction of Cyclohexanone (**9**) and 4-Nitrobenzaldehyde (**10**) using catalyst **2-5** in different emulsion systems.[a]

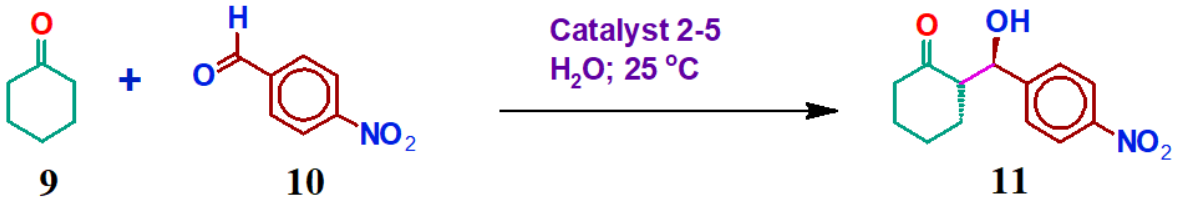


**9** **10** **11**

| Sr.No. | Emulsion Systems[a] | Amount of water [eq.] | Catalyst* | Time (h) | Yield[b] (%) | ee[c] (%) | dr[d] (%) |
|---|---|---|---|---|---|---|---|
| 1 | w/o | 25 | 2 | 24 | 90 | 96.14 | 81 |
| 2 | w/o | 25 | 3 | 24 | 91 | 95.43 | 50 |
| 3 | w/o | 25 | 4 | 12 | 99 | 97.26 | 78 |
| 4 | w/o | 25 | 5 | 16 | 99 | 97.94 | 84 |
| 5 | o/w | 84 | 2 | 24 | 90 | 96.14 | 81 |
| 6 | o/w | 84 | 3 | 24 | 99 | 95.43 | 50 |
| 7 | o/w | 84 | 4 | 10 | 99 | 91.78 | 75 |
| 8 | o/w | 84 | 5 | 14 | 99 | 97.94 | 84 |
| 9 | Water | 112 | 4 | 40 | 90 | 84.49 | 67 |
| 10 | Water | 300 | 4 | 18 | 99 | 93.52 | 58 |
| 11 | - | - | TEA[e] | 24 | 99 | 1.33 | 56 |

*10 mole% [a] The reaction was conducted with 0.33mmole of 4-nitrobenzaldehyde and 2.68mmole of cyclohexanone at 25 ºC [b] isolated yield [c] determined by chiral HPLC [d] determined by $^1$H NMR spectroscopy [e] control reaction using triethyl amine (TEA) as a catalyst.

On increasing the number of π bonds separated by sp$^3$ hybridized carbon atom (two 'lonely' π bonds) the performance of the catalyst enhanced significantly. Compound **4** gave Aldol product **11** with 99 %yield, 78 %dr and 97 %ee. It was interesting to note that reaction time dropped considerably (12 h or 10 h with w/o or o/w, respectively). This catalytic activity was maintained on insertion of third

'lonely' π bond in the hydrocarbon tail, resulting in an improvement in %dr and %ee. Compound **5** produced 99 %yield with 84 %dr and 98 %ee. The reaction was completed in 16 h for w/o and 14 h for o/w emulsion (Fig. S3).

From this performance, it is established that all the compounds (**2-5**) show good to excellent catalytic activity in o/w emulsion. These observations are in agreement with the experiments showing effect of amount of water on catalytic activity of 6 carried out by Hayashi group.[29] They showed improvement in anti/syn ratio and %ee on increasing the amount of water. In the present experiments, we had taken the amount of water 85 equiv. for o/w and 25 equiv. for w/o emulsions. Hence, present transformation mediated by o/w emulsion can be considered as '*in water*'. Above observations, infer that at least two π bonds should be present in order to achieve Aldol product with good parameters (%ee, %dr and %conversion) and responsible for lower time period.

**Table 2.** Optimization of Aldol reaction with different loading of catalyst **4** for a fixed time period.[a]

| Sr. No. | Catalyst (mole %) | Time (h) | Yield[b] (%) | ee[c] (%) | dr[d] (%) |
|---|---|---|---|---|---|
| 1 | 1 | 12 | 70.3 | 94.79 | 56 |
| 2 | 2.5 | 12 | 81.8 | 96.74 | 79 |
| 3 | 5 | 12 | 95 | 90.51 | 84 |
| 4 | 7.5 | 10 | 99 | 94.58 | 75 |
| 5 | 10 | 10 | 99 | 97.26 | 78 |

[a] The reaction was conducted with 0.33 mmole of 4-nitrobenzaldehyde and 2.68 mmole of cyclohexanone at 25 $^{o}$C [b] isolated yield [c] determined by $^{1}$H NMR spectroscopy.

For next sets of experiments, o/w system having **4** is used to evaluate activity for the same Aldol reaction. We studied %conversion of reaction mixture in a fixed time (12 h) by changing the amount of catalyst loading. It can be observed from Table 2 that the catalyst **4** maintains its activity even at 1.0 % loading in terms of enantioselectivity (94.79 % ee) with some loss in diastereoselectivity (56 % dr). Its 5% amount can be considered as 'optimum' as its results 95% yield with 90.5% ee and 86%

dr. Further, o/w system was designed, with higher content of water (112 equiv. *wrt*. p-nitrobenzaldehyde) to make greener reaction medium (Table 1), resulted only a slight decrease in % conversion (90%), %dr (67%) and %ee (85%). In the next experiment, the reaction was carried out with large amount of water (300 eq.) in presence of catalyst 4 to make the process '*in water*'. The results show that catalyst **4** is capable to carry out direct Aldol reaction maintaining the chiral induction ability in aqueous medium. Almost 74% dr with 91.78% ee in a 99% conversion resulted in aqueous medium.

Catalyst **2** was recycled by simple centrifugation at 6000 rpm while, **3-5** were recycled by washing the silica-gel used for column chromatography with methanol. The high %dr and %ee were maintained for the first three cycles. About 50% decrease in activity noted after the third cycle may be due to loss of some catalyst during the washing stage.

Mase and Barbas have proposed a mechanism for improvement in reaction yield and stereoselectivity of emulsion formed by Aldolase-type organocatalyst **7** in presence of various fatty acids.[24, 30] They proposed that the catalyst **7** forms stable emulsion with substrate cyclohexanone and fatty acid in water. The droplet formation, with organic molecules as internal phase, excludes water as separate phase responsible for shifting of equilibrium towards enamine intermediate. The enamine intermediate, being more hydrophobic than catalyst **7**, transfers to organic phase from the aqueous-organic interface where it reacts with the aldehyde via forming the stable transition state responsible for improved selectivity.

Under present situation, core solubilized cyclohexanone forms stable enamine with the proline catalytic head. The resulted enamine would be more hydrophobic than cyclohexanone, the catalyst head part would show a bending tendency towards the hydrophobic core pushing neighbouring chains away in the interfacial region. At this moment, the stability of the emulsion droplet as a whole is very important and driven by the molecular framework of the catalyst (working as emulsifier) due to π-π interactions. This interaction synergistically helps the chain to maintain the acquired conformation and directs 4-nitrobenzaldehyde (**10**) molecule to orient in an appropriate position to interact with enamine moiety (stable transition state in the hydrophobic core). Poor selectivity of the product with catalyst **3** may be due to the absence of sufficient olefinicity (only single π bond) and fails to stabilize the inner core during enamine formation. It has been observed that amount of catalyst loaded for the reaction is one of the factors that control the selectivity [31- 35] and the enantioselective reactions proceed under kinetic control when low %loading of catalyst is used. Rulli et al reported shift from kinetic to

thermodynamic controlled regime through variation in loading of Singh's catalyst **8** (0.5 to 10 mole%) in water.[17, 36- 39] However, lowering of enantioselectivity has been observed with increased loading of the catalyst with a complete loss (0 %ee) at 10% loading. This was explained in the light of thermodynamic equilibrium, established at 10% loading. Contrary to this, in the present case enantioselectivity is maintained on increasing loading (Table 1). This shows not only kinetic controlled regime but thermodynamic controlled may also produce good enantioselectivity. Therefore, the molecular structure of the catalyst besides nature of the regime plays equally important role in deciding the end output of the Aldol reaction. This may be due to the fact that catalyst, in o/w emulsion, does not allow establishment of equilibrium in reaction during the stipulated time period. Catalytic activity in terms of %selectivity was almost maintained with decrease in catalyst amount up to 2.5% (Table 2) with fair time period (10 h). However, the %dr deteriorates on further decreasing the catalyst loading to 1% with retaining the %ee. In this situation, the amount of catalyst would be insufficient to form stable emulsion. Hence, the mode of catalysis would be shifted from multi molecular aggregation to mono molecular level. This result into biphasic reaction medium with catalyst solubilized preferentially in organic phase: catalytic monomers remain present at the aqueous/organic interface such that the catalytic head towards aqueous phase while that of tail remains in the organic phase. The hydrophobic tail would adopt the plausible conformation as shown in Fig. 3 generating the stable and rigid hydrophobic cavity which serves as reaction site for Aldol acceptor. This catalytic cavity becomes more robust on insertion of each additional lonely cis- $\pi$ bond in the hydrocarbon chain. The electronic environment present inside the cavity forces to orient the aromatic aldehyde in a way that maximizes interaction with enamine moiety near catalytic head.

If above proposition is correct then only one face of the catalytic site becomes available for the donor molecules to interact and form the enamine intermediate that should be the origin of high stereo induction in the product (Fig. 4) even at lower catalyst loading. This shows that catalyst orientation near polar-non-polar interface directly influences the selectivity as observed in Table 2.

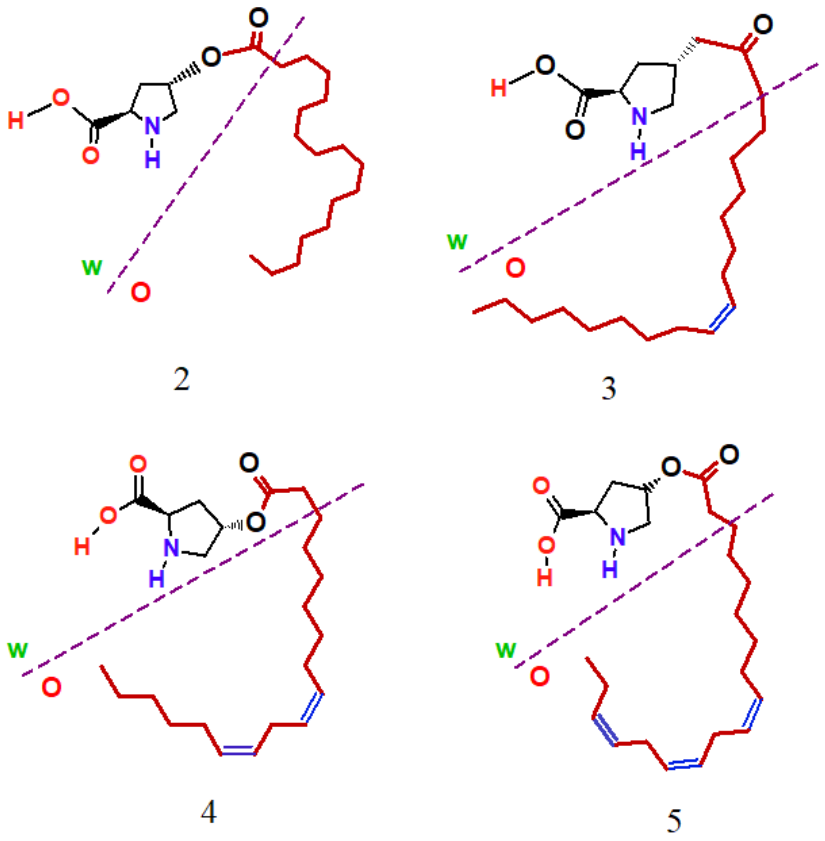


**Fig. 3.** Proposed effect of Pi bonds to the conformations of hydrocarbon chains in compounds **2-5**. Dotted line indicates interface separating water and oil phases.

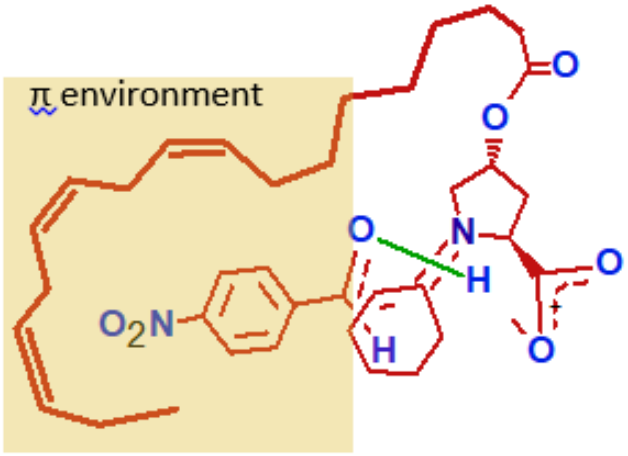


**Fig. 4.** Proposed modified List-Houk model of the transition state of the amphiphilic proline derivative catalysed Aldol reaction. Proposed π environment stabilizes the aromatic ring.

To further support these arguments, we had carried out computational studies about the possible conformations of the synthesized catalyst molecules **2-5**. Rankin et al reported the step-wise energy

changes during the proline catalysed Aldol reaction by density functional theory (DFT).[40] Present computational studies were focus to understand the role of long hydrocarbon tail with multiple olefinic bonds in the molecular framework of the catalyst to drive the Aldol reaction towards the product with specific stereochemistry. The computational quantum mechanical calculations of the synthesized catalyst molecules (**2-5**) and their intermediate structures with cyclohexanone that led to the formation of enamine followed by attack of 4-nitrobenzaldehyde were carried out by using DFT method in the gas phase. All calculations were carried out by adopting the B3LYP exchange-correlation functional and the 6-31G** basis sets coded in the computational program Gaussian 09W.[41]

The DFT computed structures along with the electrostatic potential map (ESP) of **2-5** and their intermediate enamine structure resulted from the interaction of cyclohexanone with the proline head of catalysts are shown in Fig. 5. As shown in Fig. 5, the presence of olefinic groups in the catalysts **3-5** resulted in the formation of 'pseudo hydrophobic' cavity between the reactive proline head and the hydrocarbon tail to recognize the cyclohexanone for the initiation of catalytic reaction i.e., enamine formation, first step in the Aldol reaction with formation of enamine in catalysts **3-5**, the cyclohexanone electron density overlap with the hydrocarbon tail and a circular organic framework is generated that supposed to favour the orientation of acceptor p-nitrobenzaldehyde such that its most positive region can locate over the carboxylic-OH of proline head. However, the long hydrocarbon tail in **2** remains away from the proline head due to the absence of olefinic bonds and therefore appropriate hydrophobic cavity could not generated even after interaction with cyclohexanone.

### 2.4 Computational Studies

The probable 3D structure of the complexes formed by the catalysts **2-5** with 4-Nitrobenzaldehyde (PNB) (**10**) were calculated and optimized shown in Fig. 6. PNB forms a hydrogen-bonded complex with the enamine of **2-5**, where the hydrocarbon tail envelopes the two reacting moieties and forces them to remain as near as possible for C-C bond formation. The catalysts **4** and **5** having more than one olefinic bonds in *cis*-configuration, twisted in the space to envelope the reactants better than other two catalysts. In this situation, the π-electron cloud of the hydrocarbon tail non-covalently interacts with the H-C groups of PNB (CH-π interaction) added extra stability to the intermediate. The catalyst **3** having a single π-bond in the hydrocarbon tail can envelope the reaction site and provide hydrophobic cavity, but the pi-electron cloud is more diffused and away (5.819Å) from the reaction centre, and therefore the intermediate is less favourable compared to catalyst **4** and **5**.

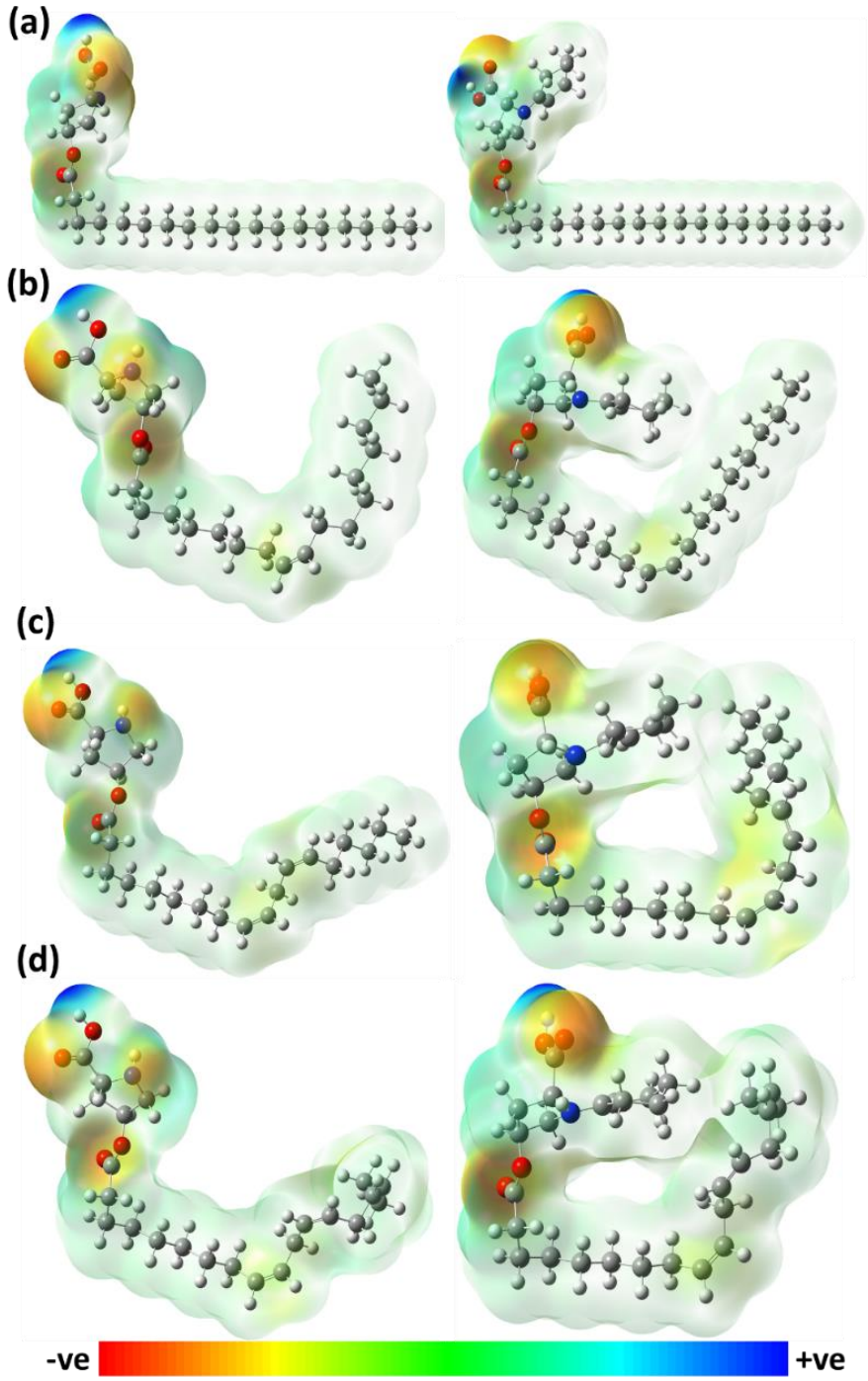


**Fig. 5.** DFT computed structures along with the electrostatic potential map of the catalysts and their corresponding adduct with cyclohexanone: (a) **2**, (b) **3**, (c) **4** and (d) **5**. The most negative region are shown in red colour whereas the most positive region in blue, the colour is extrapolated between red and blue to show the intermediate region.

In case of catalyst **2**, the calculation provides no evidence of formation of hydrophobic cavity due to the absence of olefinic bonds that stabilize the intermediates formed during the Aldol reaction. To get

further insight in to the intermediates formed between enamine and PNB, the change in interaction energy ($\Delta E_{int}$) was estimated for their reaction using the equation, $\Delta E_{int} = E_{complex} - (E_{enamine} + E_{PNB})$. With the catalysts **2-5**, the $E_{int}$ is lowered by -3.85, -2.43, -12.05 and -9.75 kJ mol-1, respectively. The estimated $E_{int}$ indicates two important results: (i) all the four catalysts energetically catalysed the Aldol reaction between cyclohexanone and PNB, and (ii) the catalysts 4 and 5 with more than one olefinic bond favour the Aldol reaction compared to other two catalysts.

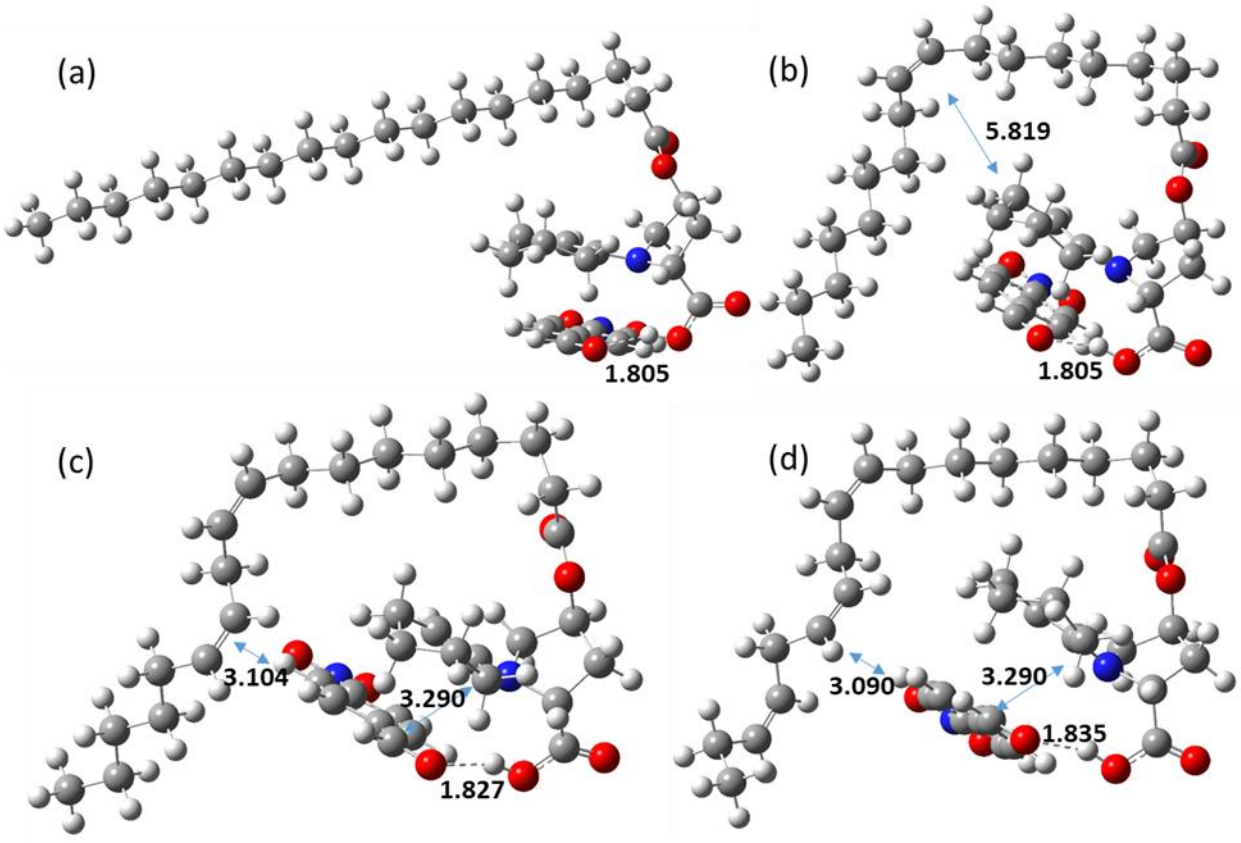


**Fig. 6.** DFT optimized transition structure formed upon interaction of PNB with the enamine adducts of the catalyst during the Aldol addition.

To complement the role of non-covalent interactions in the Aldol reaction, two model structures were optimized: Reaction-I corresponds to enamine of **5** and its complex with PNB where the long hydrocarbon tail was shorten to one carbon and Reaction-II corresponds to the adduct of reaction between enamine and acetaldehyde to understand the influence of CH-π interaction due to aromatic π-electron cloud of PNB on $E_{int}$ (Fig. 7). The $E_{int}$ for Reaction-I and II is lowered by -5.06 and -7.49 kJ $mol^{-1}$, respectively. These results indicate that the presence of long hydrocarbon tail in **2** and **3** not favouring the Aldol reaction, as the lowering in interaction energy is less as compared to the Reaction-I having no hydrocarbon tail. But the hydrocarbon tail in **4** and **5** plays an important role in accelerating

the Aldol reaction. From the Reaction-II model calculations, the $E_{int}$ is less in compared to **4** and **5** where the aromatic reactant PNB is used, and hence, it may be concluded that the aromatic π-electron clouds additionally formed non-covalent interactions with the carbon tail.

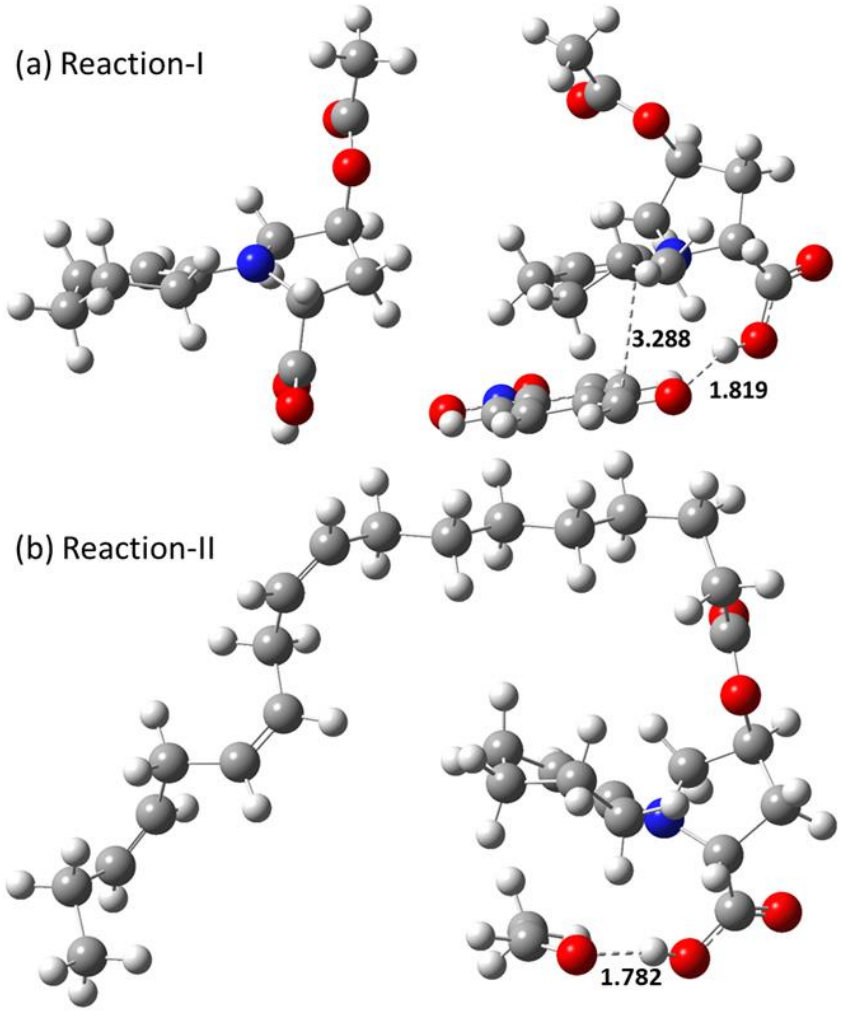


**Fig. 7.** The proposed optimized model structures to understand the influence of CH-π interaction due to aromatic π-electron cloud of PNB on $E_{int}$. Reaction-I the enamine and its complex with PNB where the long hydrocarbon tail was shorten to one carbon and Reaction-II corresponds to the adduct of reaction between enamine and acetaldehyde.

To examine the non-covalent interactions, the wave function analyses based non-covalent interactions (NCI) isosurfaces of the DFT optimized structures of enamine of **5**, its complex with PNB and the reaction-II (Fig. 8) were constructed using reduced density gradient that visualized the various kinds of non-covalent interactions like hydrogen bond, CH….π, dispersion interactions etc.[42]

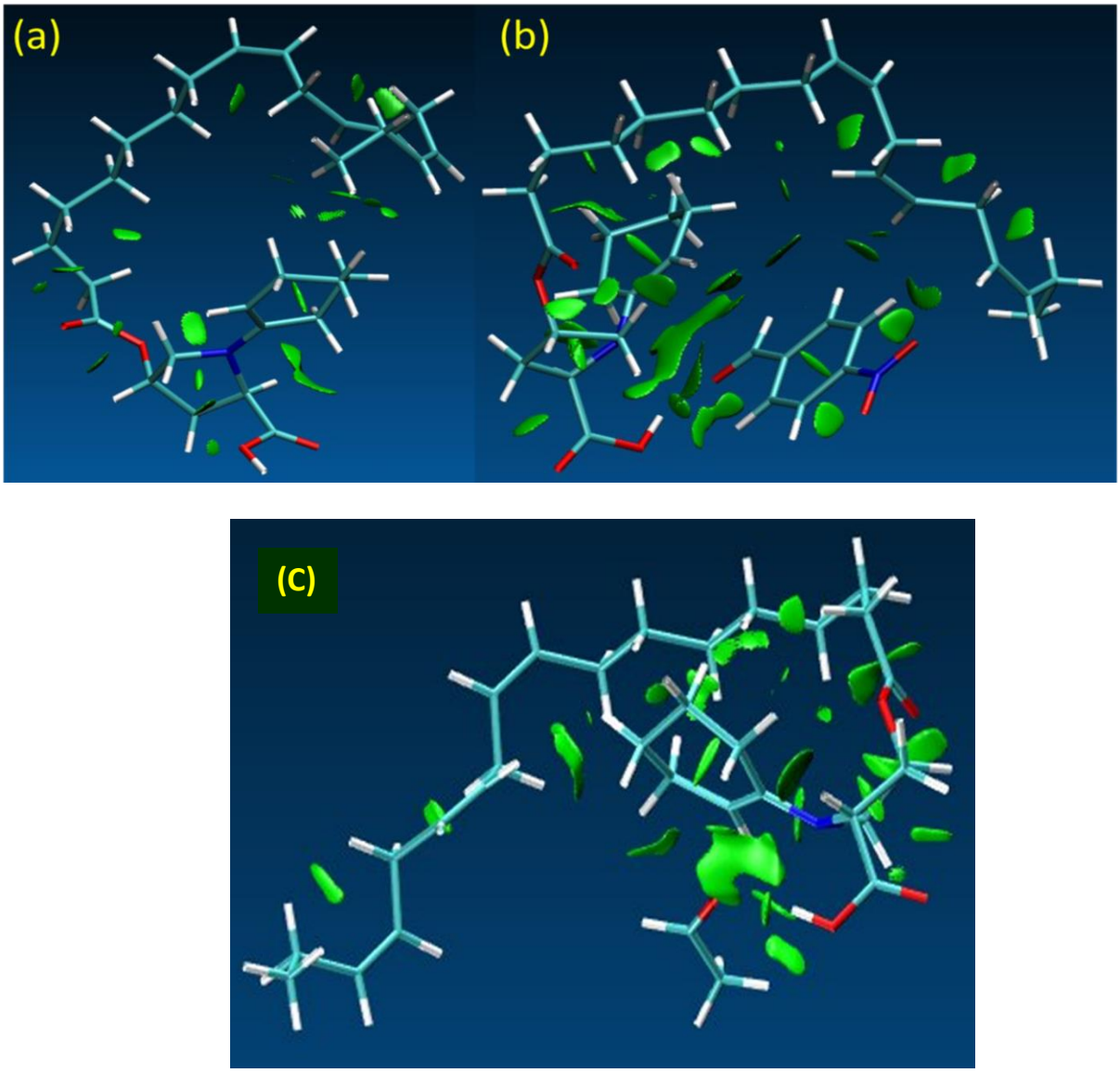


**Fig. 8.** Non-covalent interaction (NCI) isosurface plots. The green colour showing the internal attractive forces present in (a) enamine of catalyst **5** (b) its complex with PNB and (c) Reaction-II – adduct of reaction between enamine of **5** with acetaldehyde.

The twisting of the hydrocarbon tail in **5** is stabilized by various non-covalent interactions. When the enamine of **5** interacted with PNB, strong non-covalent attractive forces are generated between the cyclohexanone and the PNB along with this the intermediate is extra stabilized by CH….π interactions between the π bond present in hydrocarbon tail and the CH group of PNB. However, such CH….π interactions were not observed in Reaction-II where the PNB is replaced by acetaldehyde. So, it is established that the proline organocatalyst with remotely substituted long hydrocarbon tail having multiple olefinic bonds can do better catalysis for Aldol reaction and also favour the reaction in which the acceptor aldehyde is aromatic in nature.

## 2.5 Conclusion

We have demonstrated that chiral induction in the Aldol product is possible by creating an enzyme-like cavity in molecular framework of the amphiphilic catalyst. The Aldol reaction does not require any extra chiral auxiliaries to induce chirality in the product as, the same can be achieved due to stability of transition state of one of the stereoisomers of Aldol product in the π-environment of the cavity. Introduction of *cis*-olefinic bonds in the hydrocarbon chain serves purposes (i) it stabilizes the emulsion droplets due to π-π interactions among molecules (ii) alters the conformation of long chain and form the cavity-like shape (iii) generates the electronic environment inside the cavity stabilizes the transition state of one of the stereoisomers. On high % loading and water content, multi molecular catalysis favoured that is a large number of amphiphilic catalyst molecules form o/w type emulsion and catalysis takes place at the periphery of these emulsion droplets. While, in case of less % loading and high water content, mono molecular catalysis favoured that is catalysis takes place inside the cavity formed by each individual catalyst molecule. Stabilization of transition state of one of the stereoisomers in the π-environment of the cavity should be the reason for retaining the high enantioselectivity on increasing the amount of water in a reaction mixture. This study invites further research in the area of molecular designing and organocatalysis.

## 2.6 Characterization

FTIR (PerkinElmer, Spectrum Two) spectra of the synthesized products were obtained in the range of 400 to 4000 cm−1. The $^{1}H$ and $^{13}C$ NMR of the products were recorded on a Bruker Advance 400 MHz spectrometer using TMS as an internal standard in DMSO-$d_6$, $CD_3OD$ and $CDCl_3$. HRMS of the synthesized compounds were recorded on a XEVO-G2-S QTOF using methanol as a solvent.

***(2S, 4R)*-4-(stearoyloxy) pyrrolidine-2-carboxylic acid (2)**

Solid compound, melting point 120 ºC. $^{1}H$ NMR (400 MHz, $CD_3OD$): δ ppm- 0.87 (3H, t), 1.28 (35H, s), 1.6 (2H, br t), 2.25-2.58 (4H, m), 3.45-3.65 (2H, m), 4.55 (1H, m), 5.43 (1H, m). $^{13}C$ NMR (100 MHz, CD3OD): δ ppm- 15.2, 24.5, 26.5, 31.0, 31.6, 33.9, 35.6, 36.7, 53.1 (C-H), 60.5(C-O), 74.0 (C-O), 171.0 (C=O), 175.0 (C=O). IR (neat): ν 2915, 2849, 2709, 1748, 1741, 1635 $cm^{-1}$. HRMS: calculated for $C_{23}H_{43}NO_4$ $(M + H)^+$: 398.3265; resulted: 398.3261.

***(2S, 4R)*-4-(oleoyloxy)pyrrolidine-2-carboxylic acid (3)**

Viscous gel like compound, $^{1}$H NMR (400 MHz, $CDCl_3$): δ ppm- 0.87 (3H, t), 1.24-1.69 (26H, br m), 2.06 (2H, br m), 2.36-2.51 (4H, m), 3.57(2H, m), 4.54 (1H, br s), 5.38 (1H, br s). $^{13}$C NMR (100 MHz, $CDCl_3$): δ 14.4, 22.9-38.8, 51.7, 59.2 (C-H), 64.6 (C-O), 72.0 (C-O), 130.0 (C=C), 173.0 (C=O), 179.0 (C=O). IR (neat): ν 2924, 2854, 1738, 1678, 1634 $cm^{-1}$. HRMS: calculated for $C_{23}H_{41}NO_4$ $(M + H)^+$: 396.3108; resulted: 396.3109. UV( $CH_3OH$): $\lambda_{max}$ 214 nm. Dynamic light scattering (size distribution by hydrodynamic volume, 25 ºC): 331.6 d.nm.

***(2S, 4R)*-4-(((9Z, 12Z)-octadeca-9, 12-dienoyl) oxy) pyrrolidine-2-carboxylic acid (4)**

Viscous gel like compound, $^{1}$H NMR (400 MHz, $CDCl_3$): δ ppm- 0.87 (3H, t), 1.24-1.69 (26H, br m), 2.06 (2H, br m), 2.36-2.51 (4H, m), 3.57(2H, m), 4.54 (1H, br s), 5.38 (1H, br s). $^{13}$C NMR (100 MHz, $CDCl_3$): δ ppm- 14.4, 22.9-31.8 (C-H), 128.4 (C=C), 130.5 (C=C). IR (neat): ν 2924, 2854, 1738, 1678, 1634 $cm^{-1}$. HRMS: calculated for $C_{23}H_{39}NO_4$ $(M+H)^+$: 394.2952; resulted: 394.2953. UV (CH3OH): λmax 211, 267 nm. Dynamic light scattering (size distribution by hydrodynamic volume, 25 ºC): 1186 d.nm.

***(2S, 4R)*-4-(((9Z, 12Z, 15Z)-octadeca-9, 12, 15-trienoyl) oxy) pyrrolidine-2-carboxylic acid (5)**

Viscous gel like compound, $^{1}$H NMR (400 MHz, $CDCl_3$): δ ppm- 0.87 (3H, t), 1.24-1.69 (26H, br m), 2.06 (2H, br m), 2.36-2.51 (4H, m), 3.57(2H, m), 4.54 (1H, br s), 5.38 (1H, br s). $^{13}$C NMR (100 MHz, $CDCl_3$): δ ppm- 14.4, 20.9-34.3 (C-H), 127.4 (C=C), 128.5 (C=C), 132.3 (C=C), 173.5 (C=O). IR (neat): ν 2924, 2854, 1738, 1678, 1634 $cm^{-1}$. HRMS: calculated for $C_{23}H_{37}NO_4$ (M + H)+: 392.2795; resulted: 392.2796. UV ($CH_3OH$): λmax 210, 268, 314 nm. Dynamic light scattering (size distribution by hydrodynamic volume, 25 ºC): 1800 d.nm.

**(*R*)-2-((*S*)-hydroxy (4-nitrophenyl) methyl) cyclohexan-1-one (The model Aldol product)**

$^{1}$H NMR (400 MHz, DMSO-$d_6$): δ ppm- 1.15-1.23 (2H, m), 1.55-1.89 (4H, m), 2.80 (1H, br s), 2.50 (2H, br s), 2.71 (1H, m), 5.09 (1H, d), 5.23 (1H, s), 5.47 (1H, d), 5.54 (1H, s),7.61(2H, d), 8.18 (2H, d). % ee (by chiral HPLC) on a chiralpak AD-H column, λ = 210 nm, iPrOH/hexane, 20:80, 0.7 mL min-1; $t_R$ = 17.8 min (major), 14.2 min (minor).

### 2.6.1. Optical microscopic studies

Optical microscopic (OM) images and dynamic light scattering (DLS) analysis were carried out. For the purpose, 4 mg (0.01 mmole) of catalyst **(3-5)** was mixed in 2 mL cyclohexanone and the mixture was stirred. On clear solution, 1 mL of water was added and the mixture was stirred vigorously for 15 min to form emulsion. Immediately the photographs were taken. Similar results were observed when these systems were kept under stirring (similar rpm as the actual reaction) and observed after 24 h.

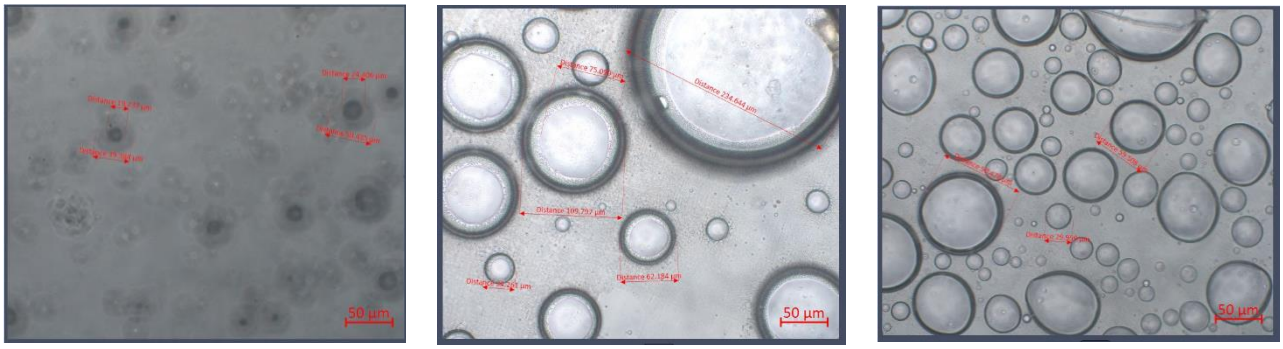


**S1** **S2** **S3**

**Fig. S1/S2/S3.** Optical microscopy image of w/o emulsion using compound **3, 4** and **5.**

### 2.6.2. Dynamic light scattering analysis

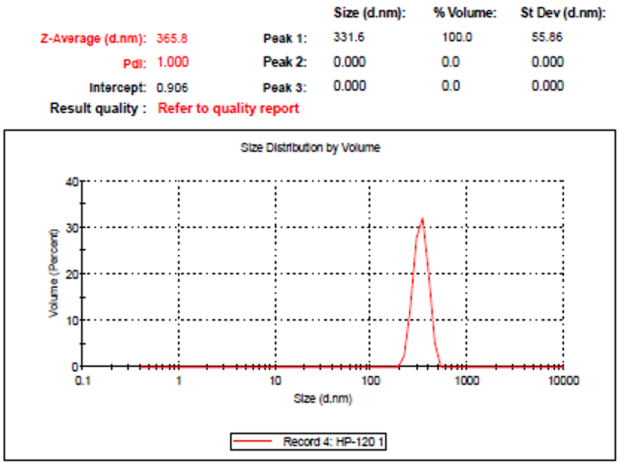


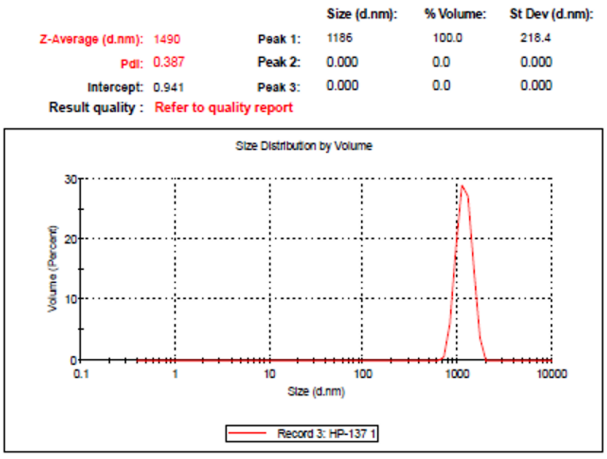


**S4** **S5**

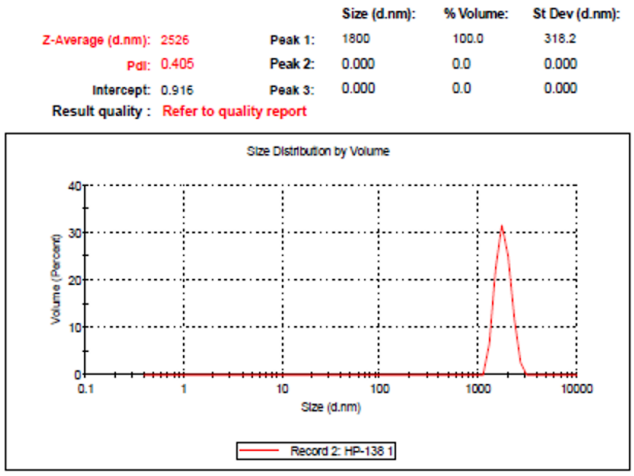


**S6**

**Fig. S4/S5/S6.** Dynamic light scattering analysis of w/o emulsion using compound **3, 4** and **5.**

### 2.6.3. Emulsion stability analysis

For w/o type, 4 mg (0.01 mmole) of catalyst (**3-5**) was mixed in 2 mL cyclohexanone and the mixture was stirred. On clear solution, 1 mL of water was added and the mixture was stirred vigorously for 15 min. The DLS study and optical microscopy was performed on these systems. For o/w type, 4 mL water was added and similar procedure was performed.

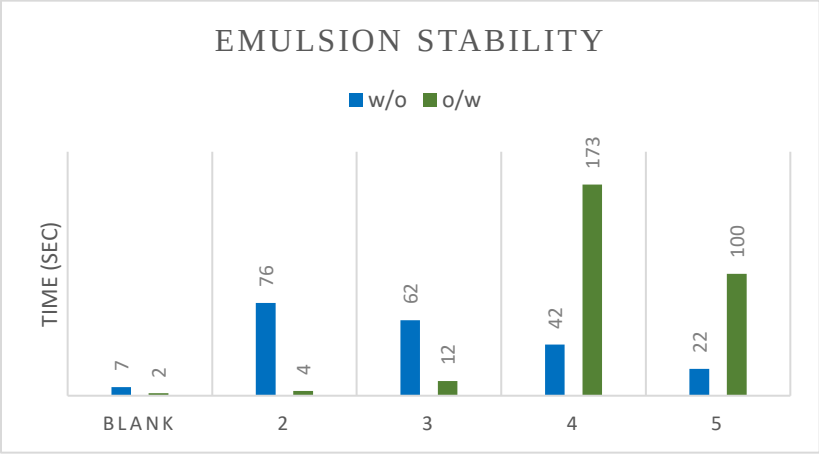


**Chart 1**. Comparison of emulsion (cyclohexanone and water) stability with **2-5** compounds.

Stability time of different emulsion systems which formed by catalyst **2-5** (0.01 mmole catalyst, 1000 µl of water in 2000 µl of cyclohexanone for w/o system and vice versa for o/w system). The time for initiation of phase separation was recorded for each system. Blank was considered as without catalytic compound. When organic transformation carried out by using these emulsion system as micro-

reactors, under continuous stirring at high rpm prevents the droplet to coalesce and forms the separate phase confirmed by studying optical micrographs of the system at various reaction stages.

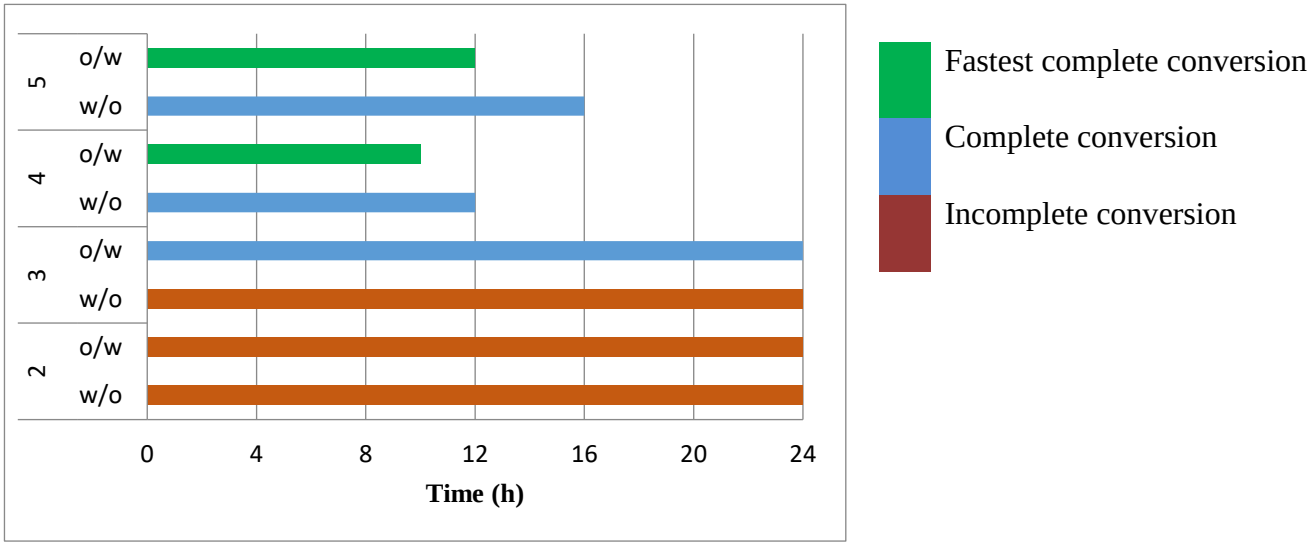


**Fig. S7**. Effect of 10 mole% loaded catalyst **2-5** on the model Aldol reaction kinetics (time reported is within the error of ± 0.5 h).

### 2.6.4. Spectroscopic analysis of compound 2-5

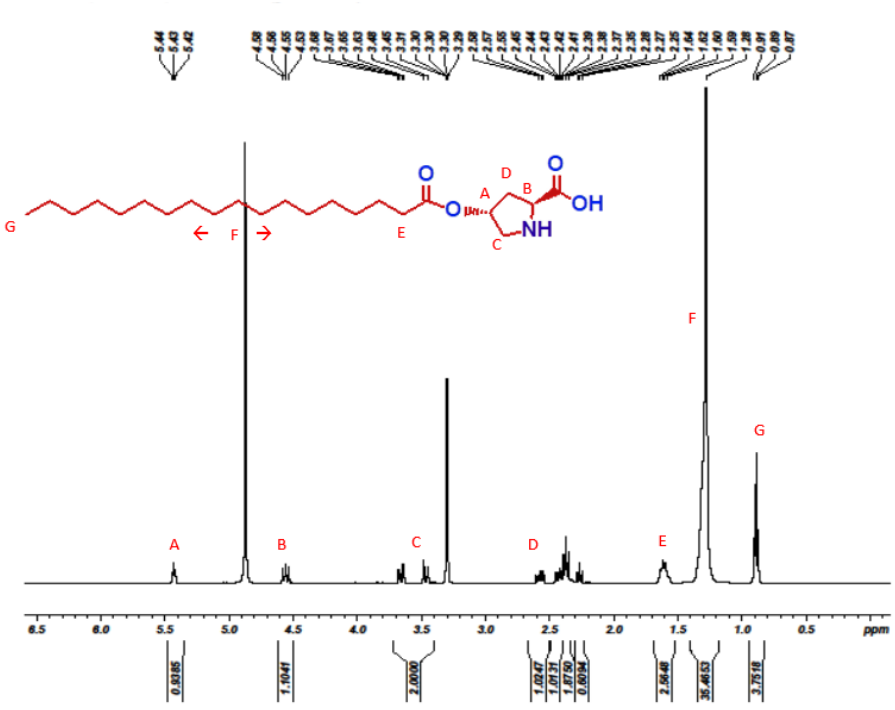


**Fig. S8.** $^{1}$H NMR of (*2S, 4R*)-4-(stearyloxy) pyrrolidine-2-carboxylic acid (**2**).

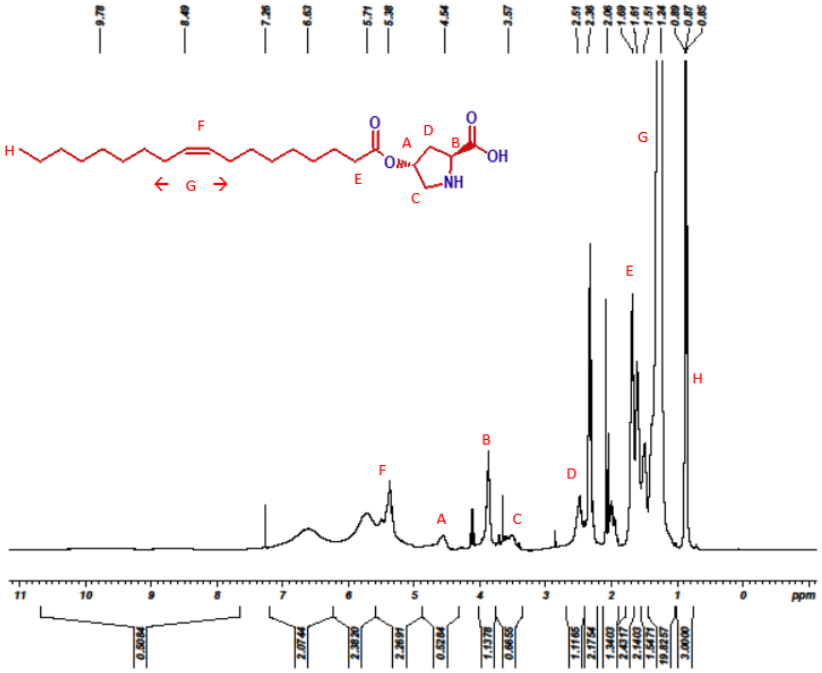

**Fig. S9**. $^{1}$H NMR of (*2S, 4R*)-4-(oleoyloxy) pyrrolidine-2-carboxylic acid (**3**).

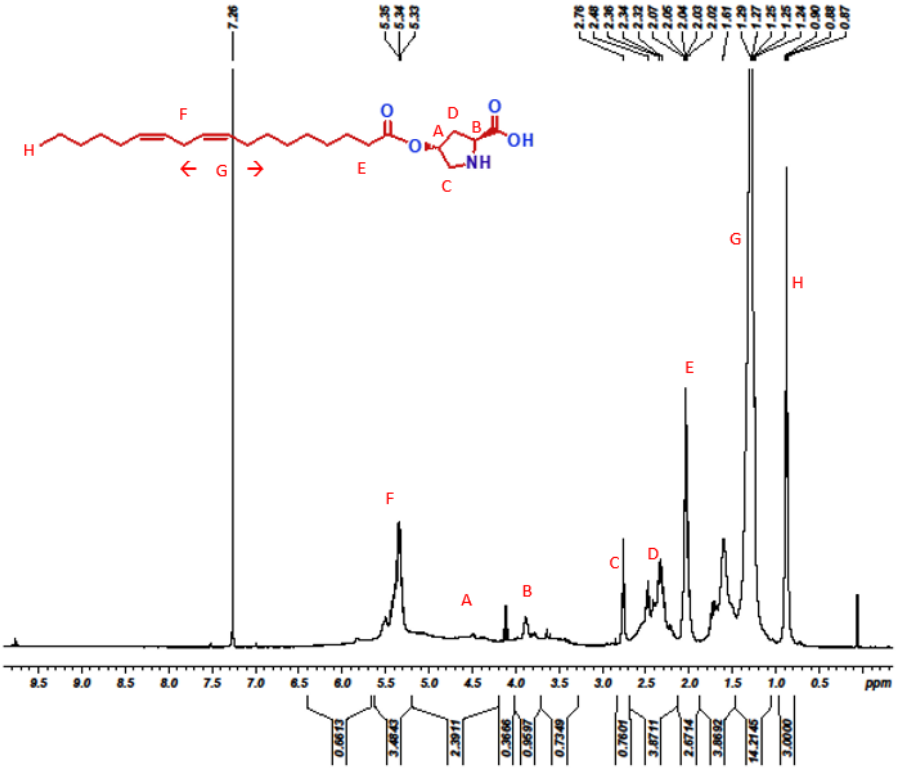

**Fig. S10**. $^{1}$H NMR of (*2S, 4R*)-4-(((9Z, 12Z)-octadeca-9, 12-dienoyl) oxy) pyrrolidine-2-carboxylic acid (**4**).

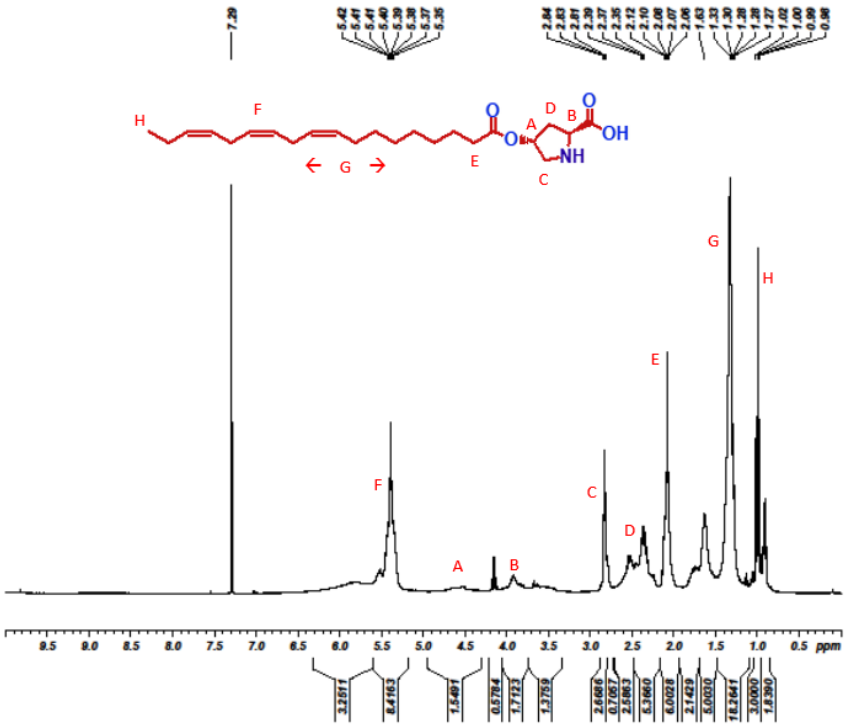


**Fig. S11.** [1]H NMR of (*2S, 4R*)-4-(((9Z, 12Z, 15Z)-octadeca-9, 12, 15-trienoyl) oxy) pyrrolidine-2-carboxylic acid (**5**).

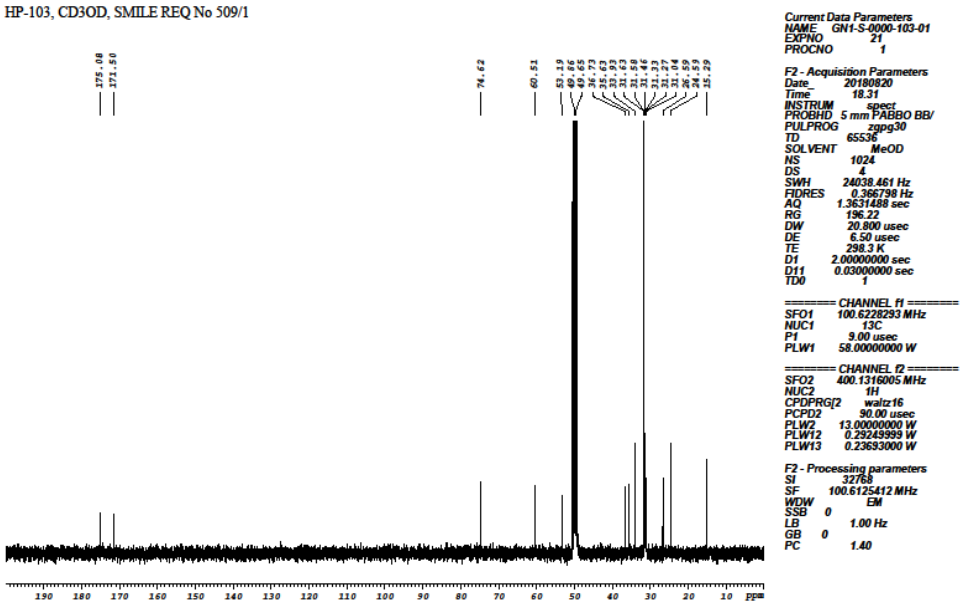


**Fig. S12.** [13]C NMR of (*2S, 4R*)-4-(stearoyloxy) pyrrolidine-2-carboxylic acid (**2**).

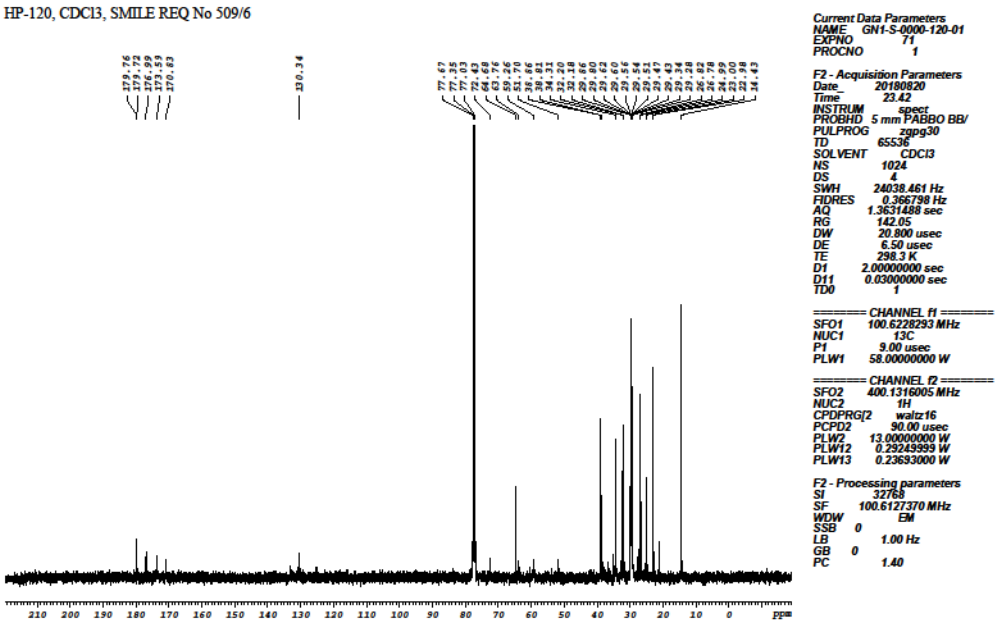


**Fig. S13.** $^{13}$C NMR of (*2S, 4R*)-4-(oleoyloxy) pyrrolidine-2-carboxylic acid (**3**).

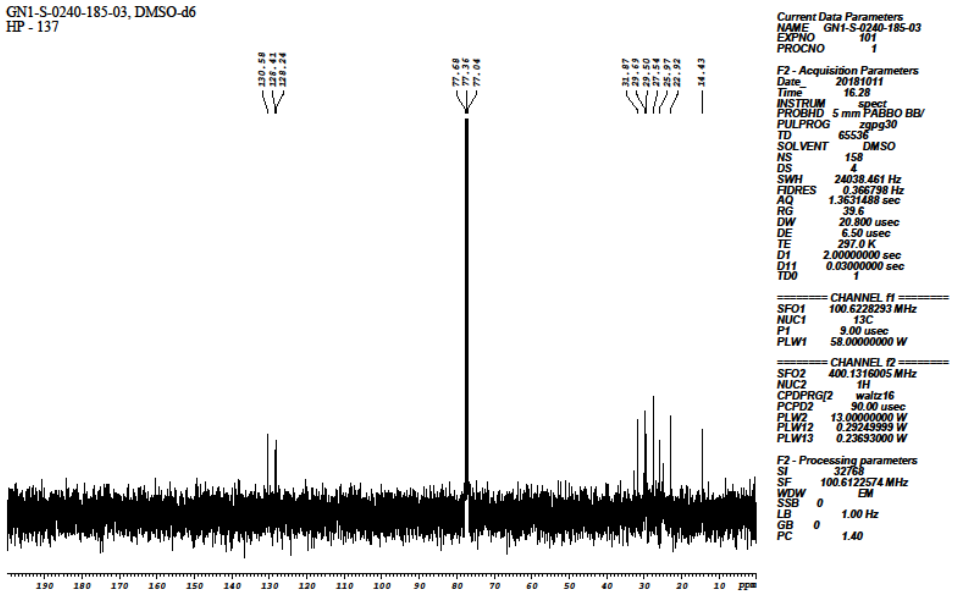


**Fig. S14.** $^{13}$C NMR of (*2S, 4R*)-4-(((9Z, 12Z)-octadeca-9, 12-dienoyl) oxy) pyrrolidine-2-carboxylic acid (**4**).

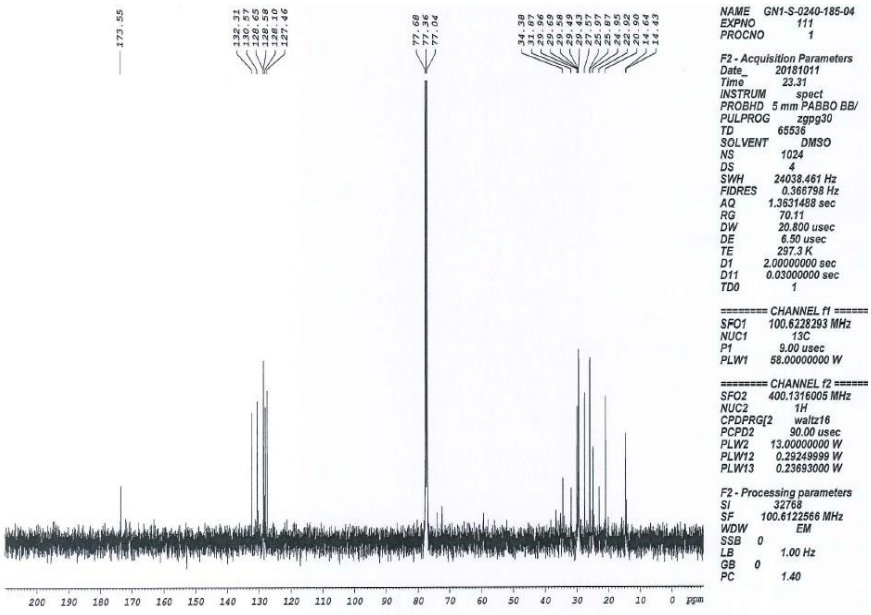


**Fig. S15.** $^{13}$C NMR of (*2S, 4R*)-4-(((9Z, 12Z, 15Z)-octadeca-9, 12, 15-trienoyl) oxy) pyrrolidine-2-carboxylic acid (**5**).

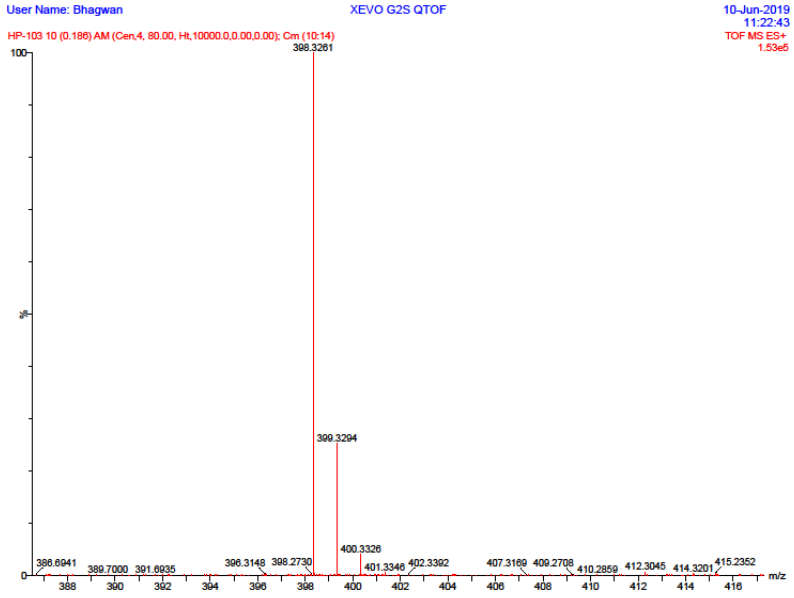


**Fig. S16.** HRMS of (*2S, 4R*)-4-(stearoyloxy) pyrrolidine-2-carboxylic acid (**2**).

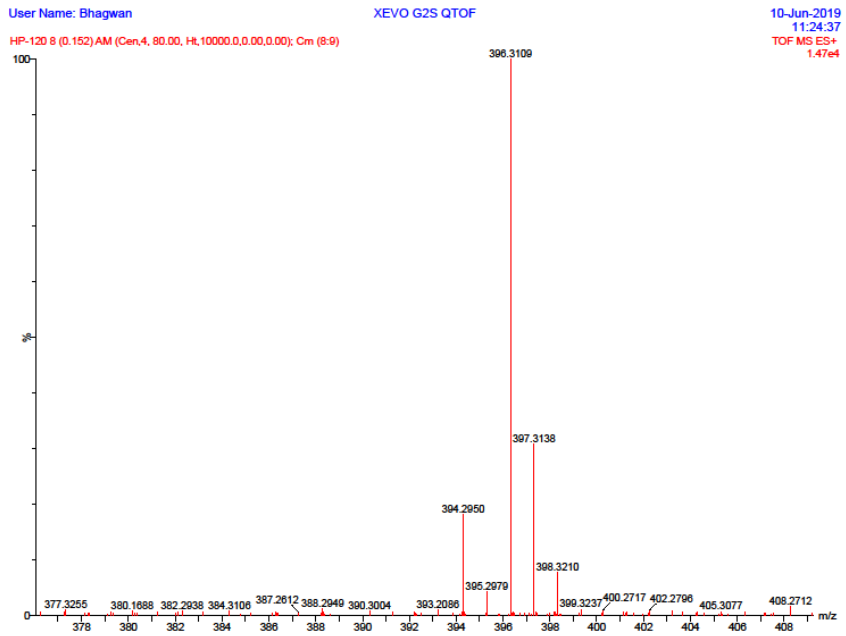


**Fig. S17.** HRMS of (*2S, 4R*)-4-(oleoyloxy) pyrrolidine-2-carboxylic acid (**3**).

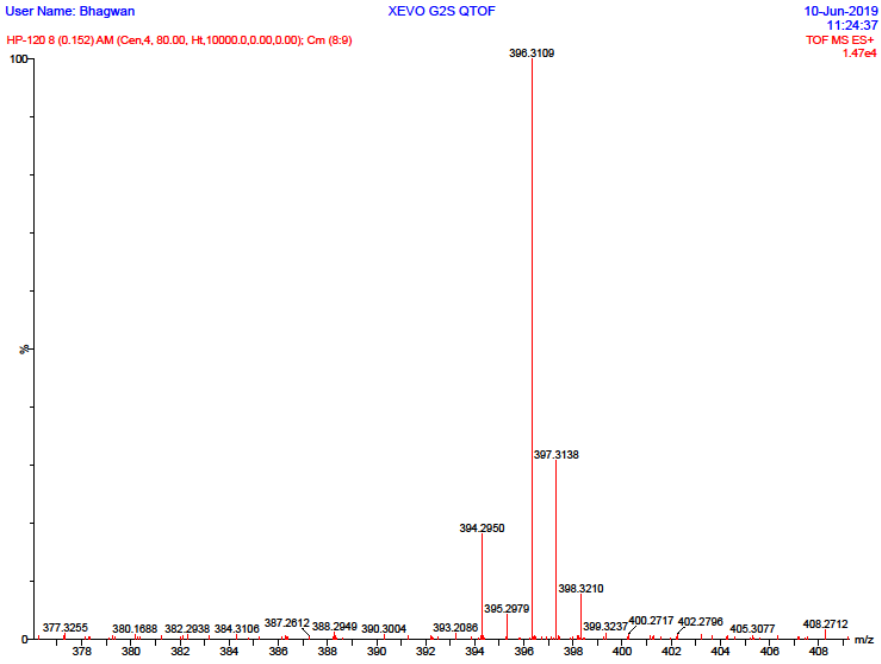


**Fig. S18.** HRMS of (*2S, 4R*)-4-(((9Z, 12Z)-octadeca-9, 12-dienoyl) oxy) pyrrolidine-2-carboxylic acid (**4**).

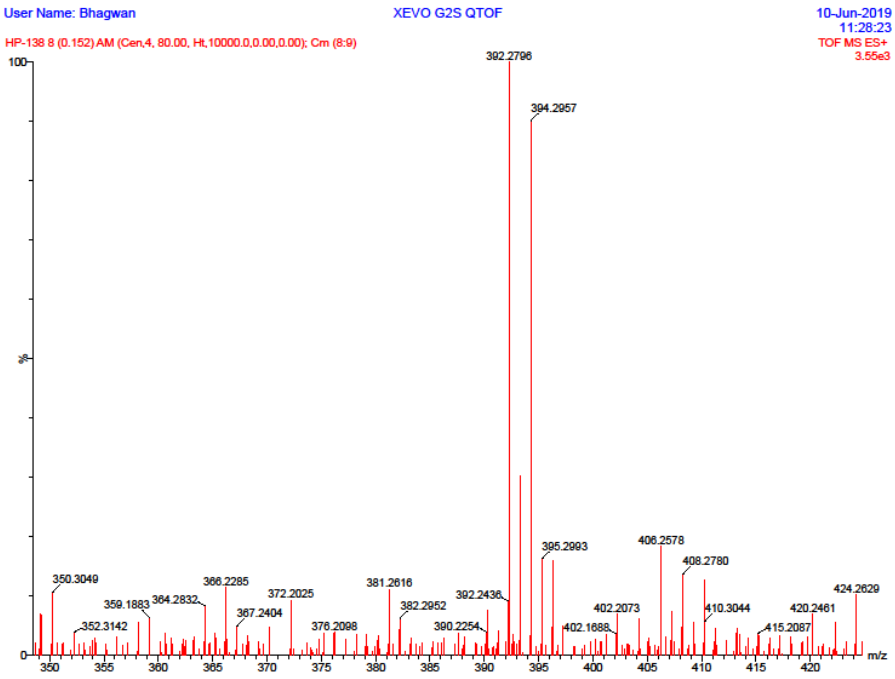


**Fig. S19.** HRMS of (*2S*, *4R*)-4-(((9Z, 12Z, 15Z)-octadeca-9, 12, 15-trienoyl) oxy) pyrrolidine-2-carboxylic acid (**5**).

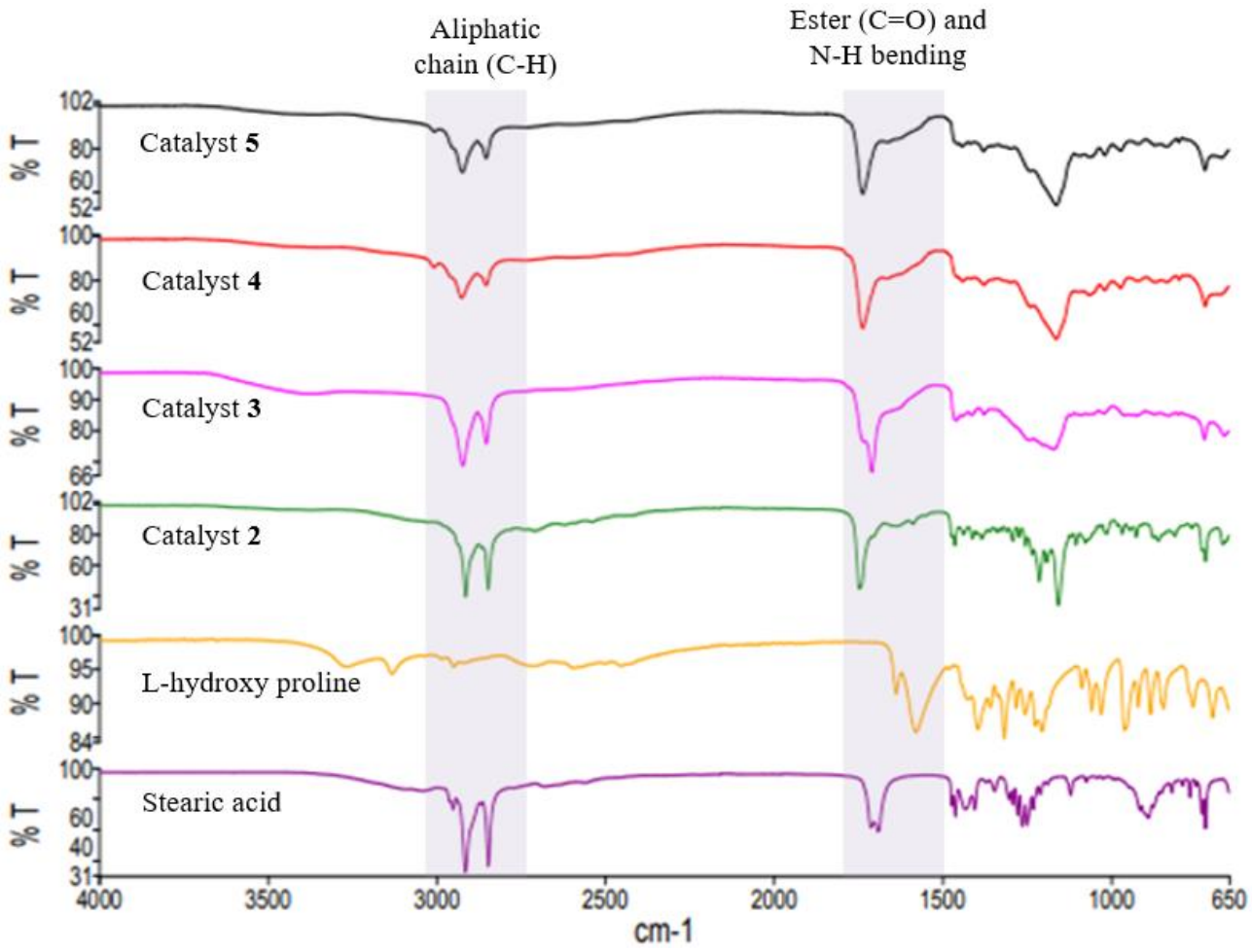


**Fig. S20.** FTIR Analysis of Compound **2-5** and comparison with 4-hydroxy proline and stearic acid.

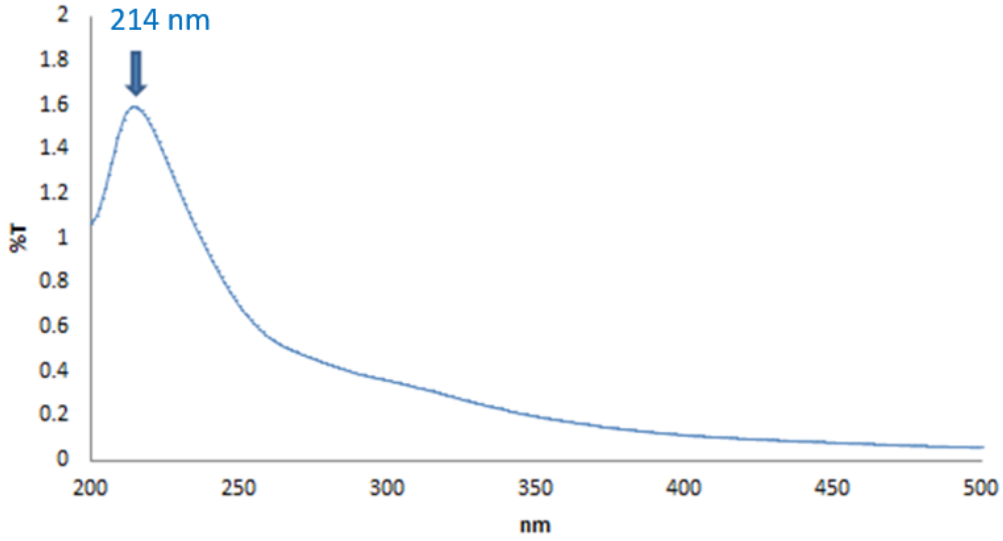


**Fig. S21.** UV analysis of (*2S*, *4R*)-4-(oleoyloxy) pyrrolidine-2-carboxylic acid (**3**).

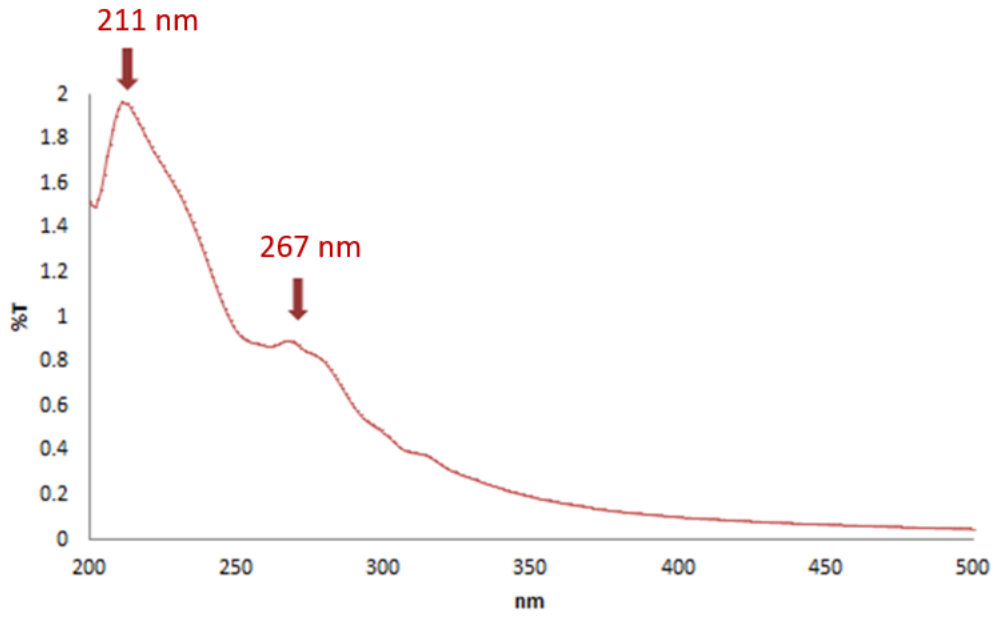


**Fig. S22.** UV analysis of (*2S*, *4R*)-4-(((9Z, 12Z)-octadeca-9, 12-dienoyl) oxy) pyrrolidine-2-carboxylic acid (**4**).

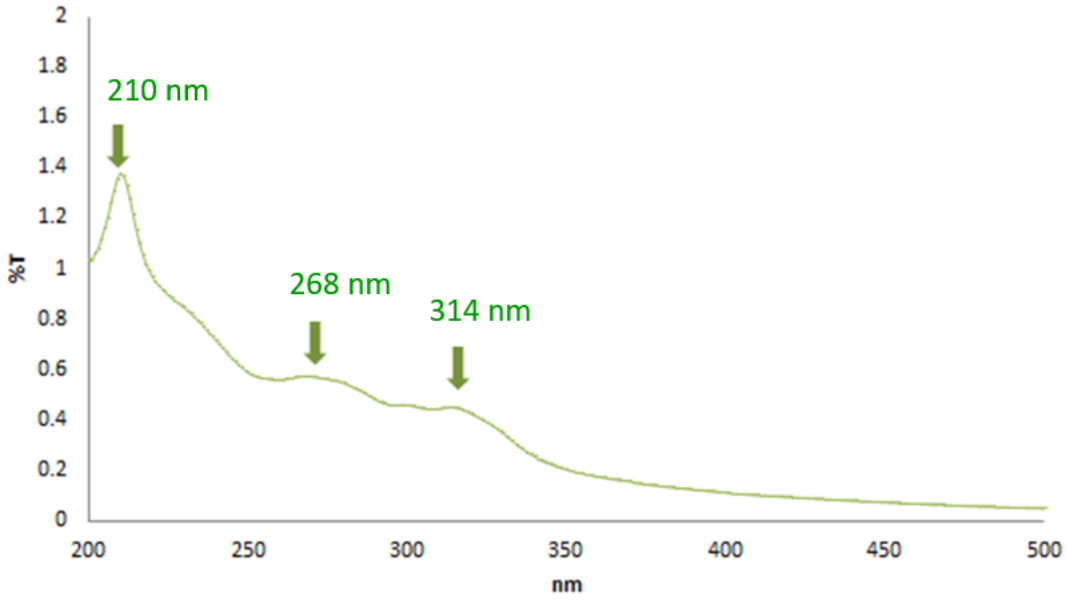


**Fig. S23.** UV analysis of (*2S*, *4R*)-4-(((9Z, 12Z, 15Z)-octadeca-9, 12, 15-trienoyl) oxy) pyrrolidine-2-carboxylic acid (**5**).

### 2.6.5. NMR spectroscopy of the model Aldol product

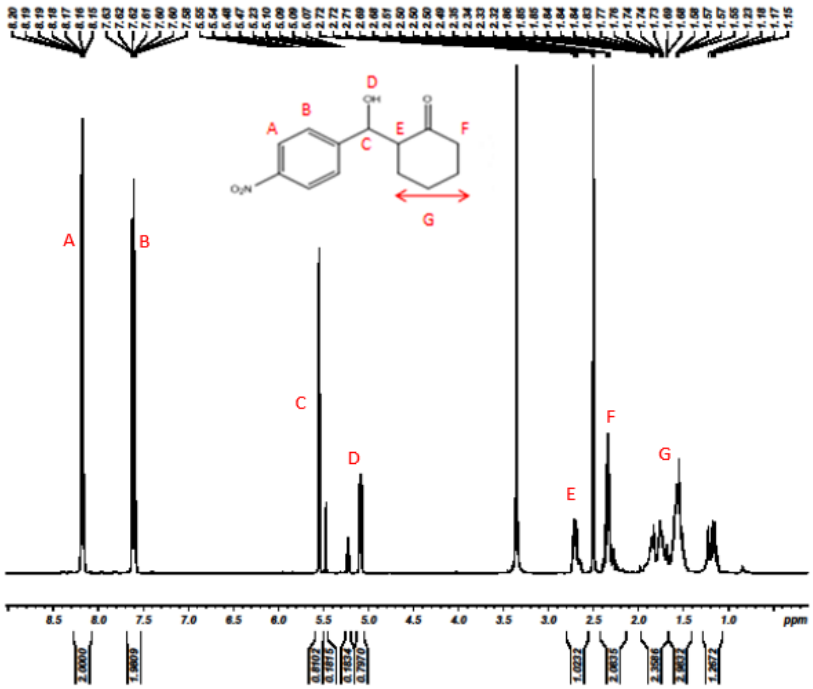


**Fig. S24.** $^{1}$H NMR of 2-hydroxy (4-nitrophenyl) methyl) cyclohexan-1-one (Table 1, entry 1).

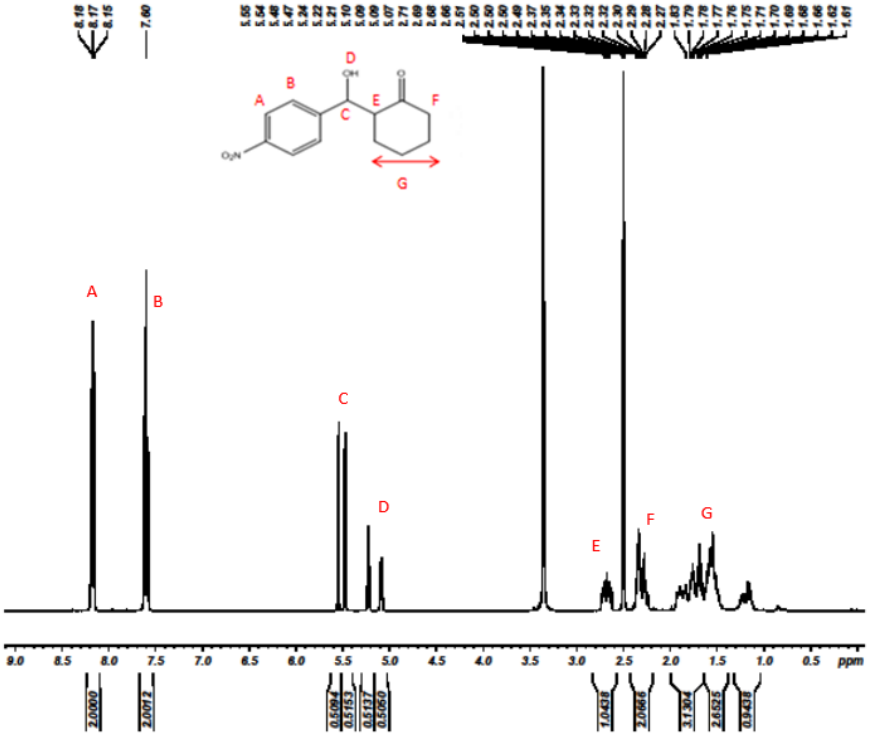


**Fig. S25.** $^{1}$H NMR of 2-hydroxy (4-nitrophenyl) methyl) cyclohexan-1-one (Table 1, entry 2).

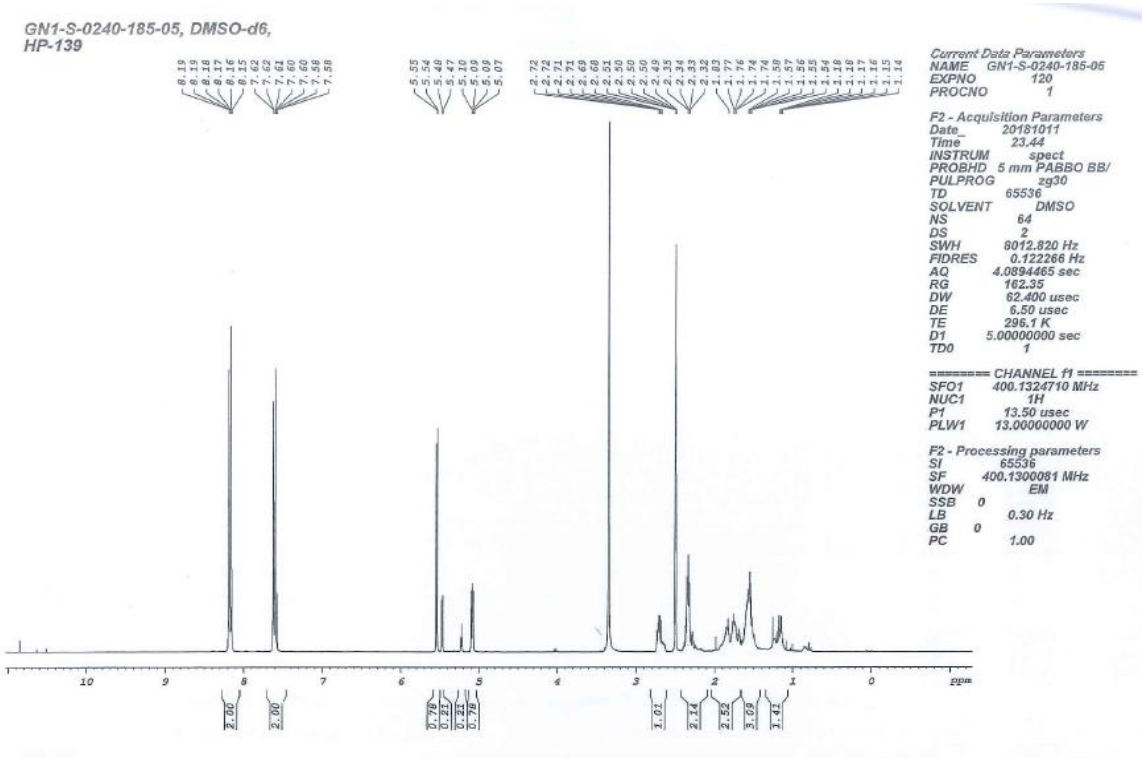


**Fig. S26.** [1]H NMR of 2-hydroxy (4-nitrophenyl) methyl) cyclohexan-1-one (Table 1, entry 3).

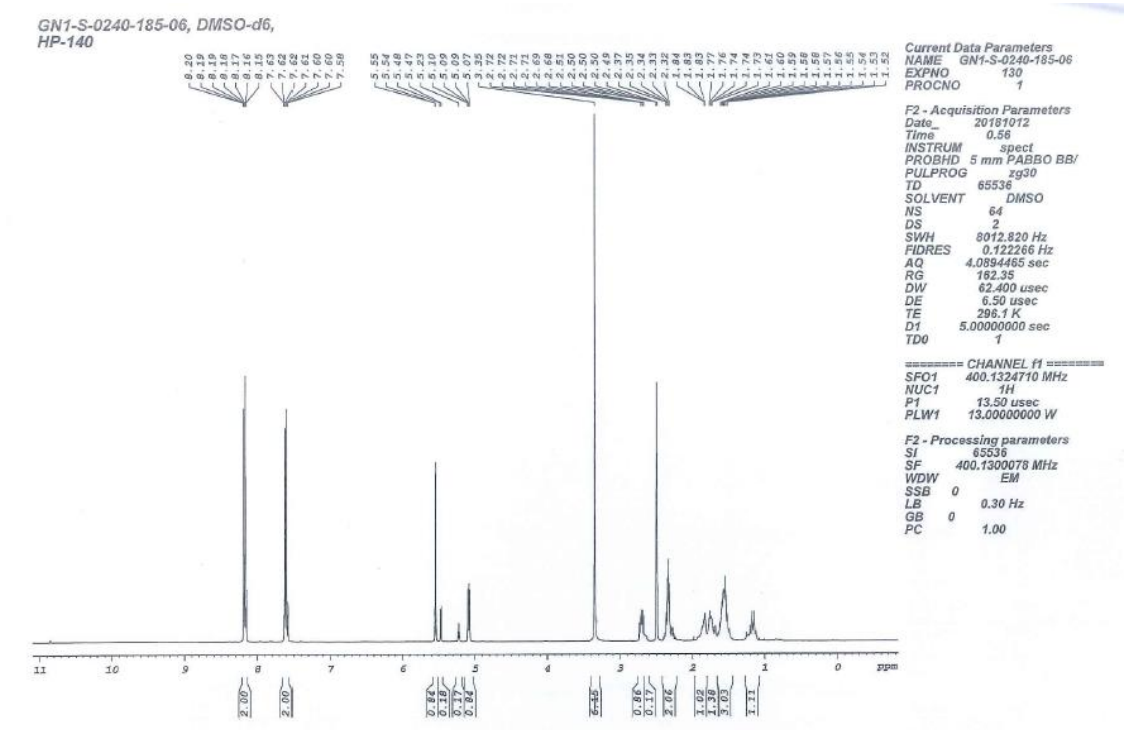


**Fig. S27.** [1]H NMR of 2-hydroxy (4-nitrophenyl) methyl) cyclohexan-1-one (Table 1, entry 4).

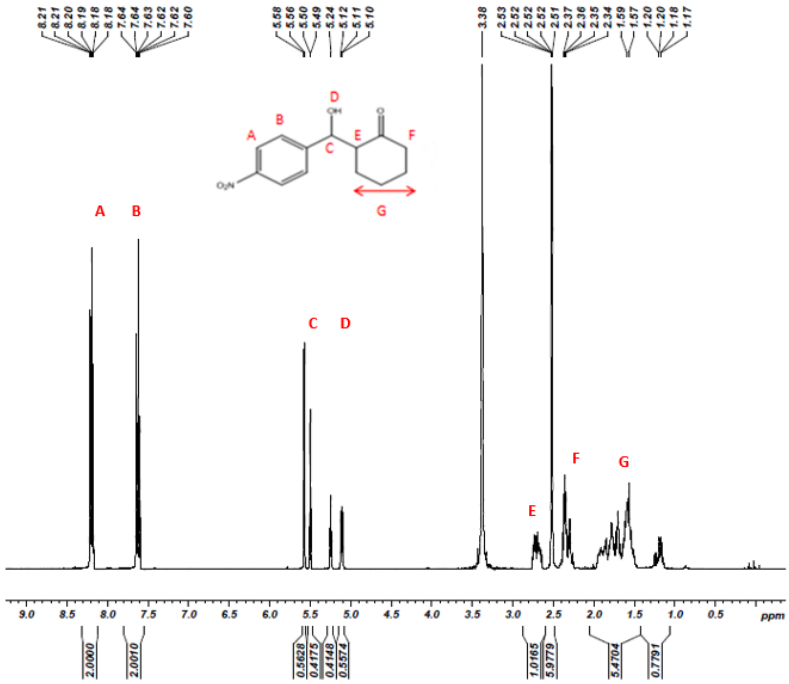

**Fig. S28**. $^{1}$H NMR of 2-hydroxy (4-nitrophenyl) methyl) cyclohexan-1-one (Table 2, entry 1).

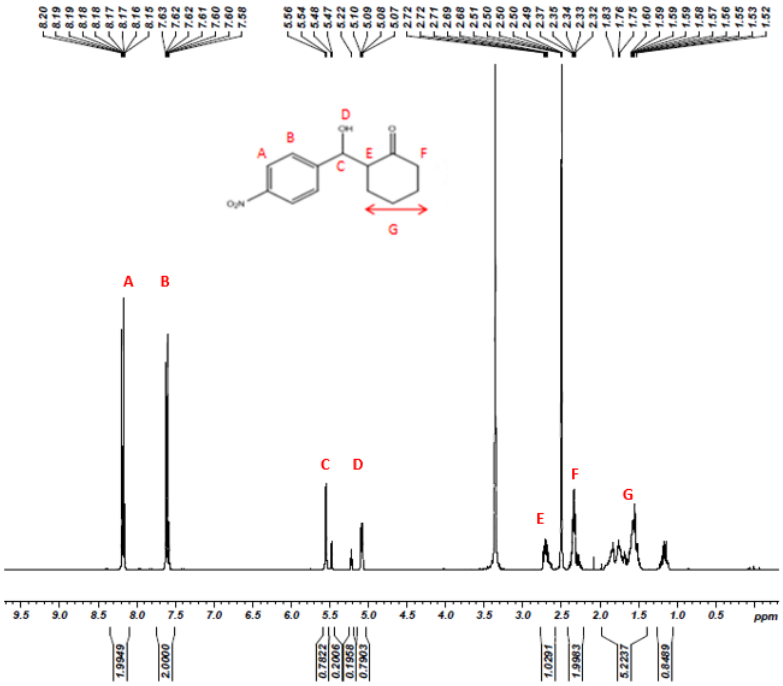

**Fig. S29.** $^{1}$H NMR of 2-hydroxy (4-nitrophenyl) methyl) cyclohexan-1-one (Table 2, entry 2).

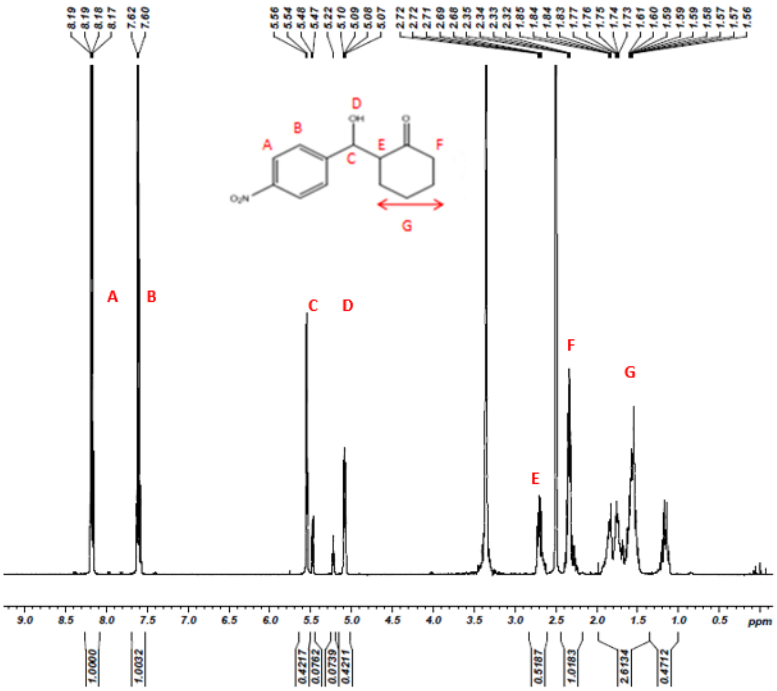

**Fig. S30.** [1]H NMR of 2-hydroxy (4-nitrophenyl) methyl) cyclohexan-1-one (Table 2, entry 3).

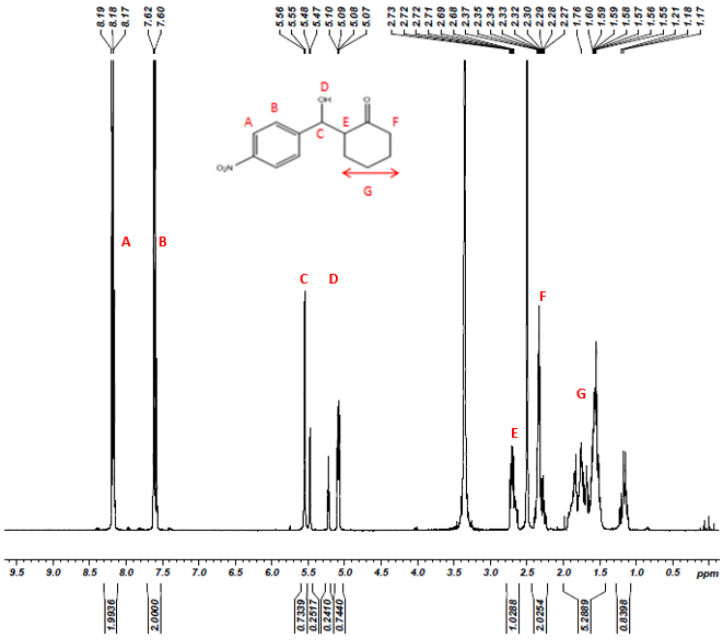

**Fig. S31**. [1]H NMR of 2-hydroxy (4-nitrophenyl) methyl) cyclohexan-1-one (Table 2, entry 4).

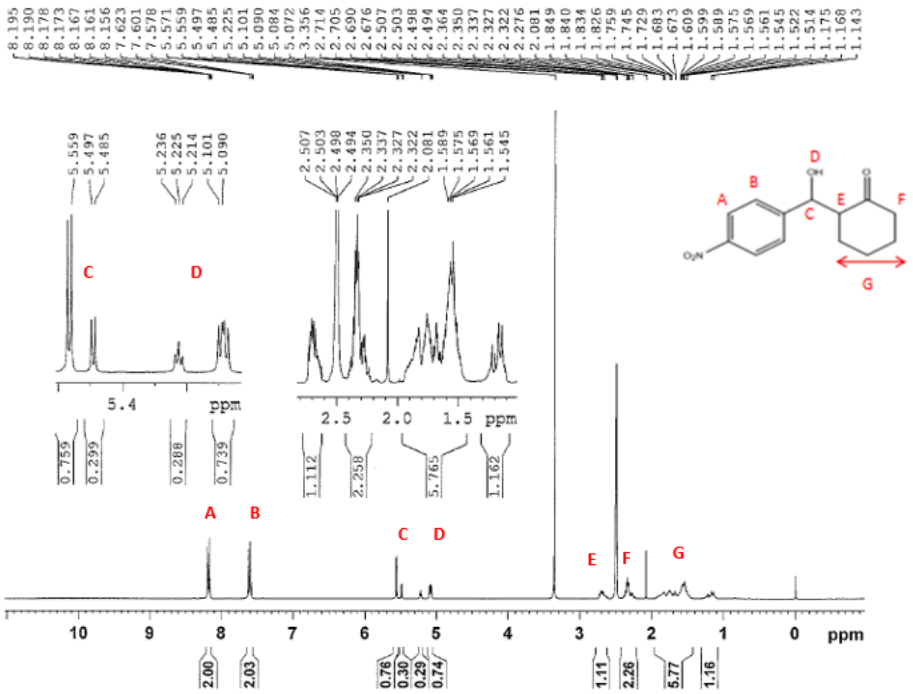

**Fig. S32**. $^{1}$H NMR of 2-hydroxy (4-nitrophenyl) methyl) cyclohexan-1-one (Table 1, entry 7).

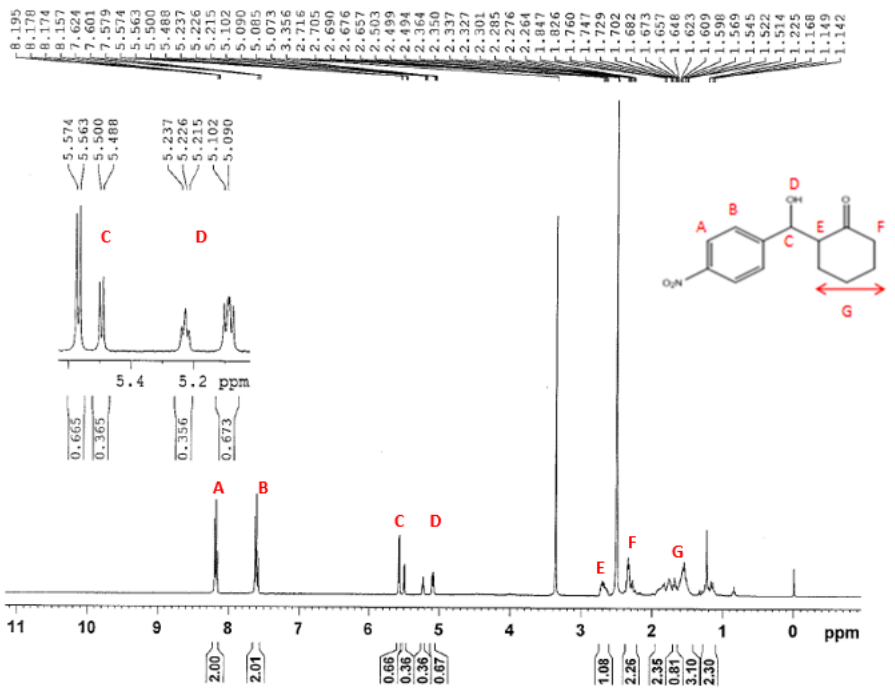

**Fig. S33.** $^{1}$H NMR of 2-hydroxy (4-nitrophenyl) methyl) cyclohexan-1-one (Table 1, entry 9).

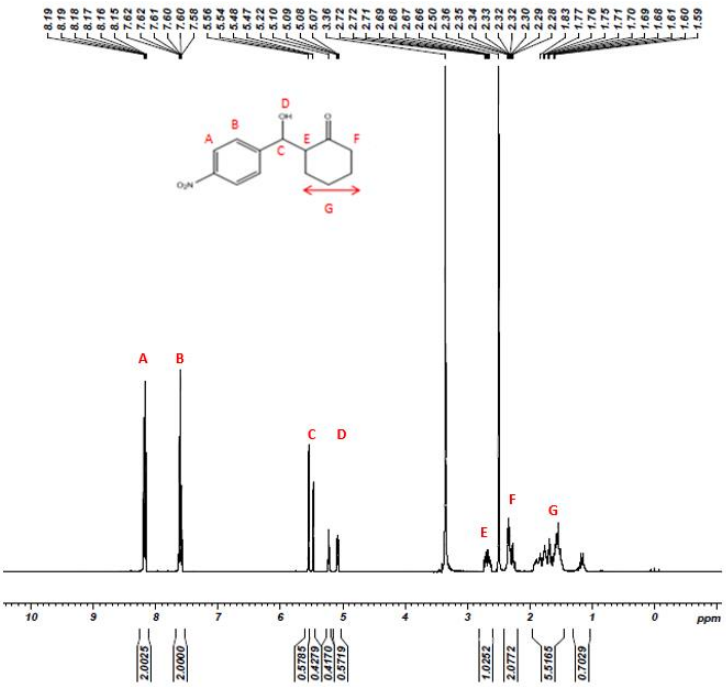

**Fig. S34.** [1]H NMR of 2-hydroxy (4-nitrophenyl) methyl) cyclohexan-1-one (Table 1, entry 10).

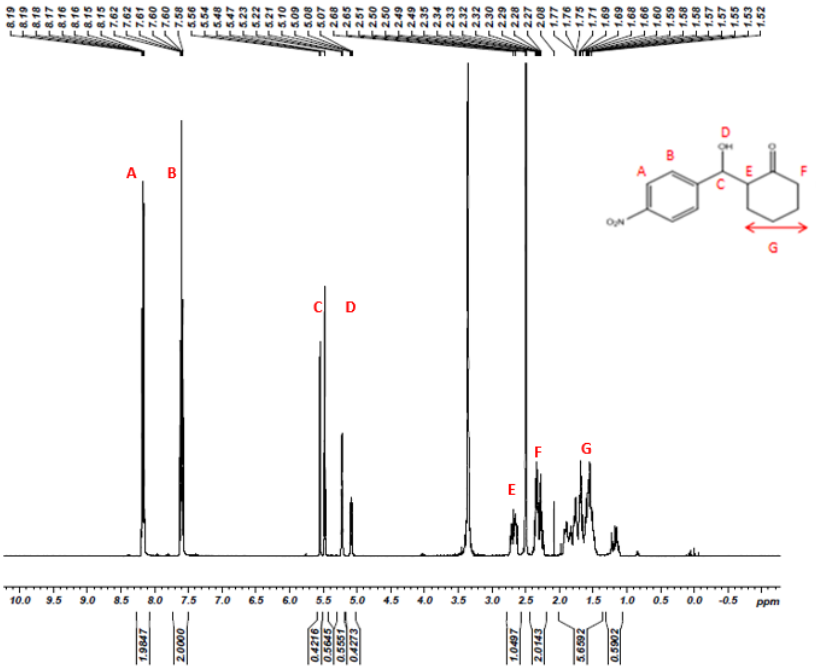

**Fig. S35.** [1]H NMR of 2-hydroxy (4-nitrophenyl) methyl) cyclohexan-1-one (Table 1, entry 11).

### 2.6.6 Aldol product: enantiomeric excess determination by using chiral HPLC Analysis.

The enantiomeric excess (ee) of Aldol product (**11**) was determined by chiral-phase HPLC analysis. The absolute configuration of Aldol product **11** was extrapolated by comparison of the HPLC-data with those of **11 (**four stereoisomers**)** whose absolute configuration is known.

| **Structure** | **CAS No.** | **HPLC [a]** | | | |
|---|---|---|---|---|---|
| | | **column** | **eluent** | ***syn*** **$t_R$ (min)** | ***anti*** **$t_R$ (min)** |
| 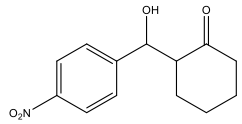 | (2 R,1' S)-501417-31-8<br>(2 S,1' S)-501417-28-3<br>(2 S,1' R)-351533-35-2<br>(2 R,1' R)-349628-69-9<br>rel-(2 S,1' R)-71444-30-9<br>rel-(2 R,1' R)-71444-29-6<br>racemic-61235-16-3 | Chiralpak AD-H | n-Hexane:*i*-PrOH = 80:20 | 21.767 (minor)<br>23.733 (major) | 25.708 (2S, 1'R)<br>32.875 (2R, 1'S) |

*[a] Flow rate = 0.5 mL/min, λ=254 nm.* (*Ref.* N. Mase, Y. Nakai, N. Ohara, H. Yoda, K. Takabe, F. Tanaka, C. F. Barbas III, *J. Am. Chem. Soc.* **2006**, *128*, 734-735).

**Note:** In present study, the flow rate during chrial HPLC analysis was set as 0.7 mL/min and λ = 210 nm. This change in parameters alters the $t_R$ of stereoisomers. However, the pattern of product separation is considered as remains same.

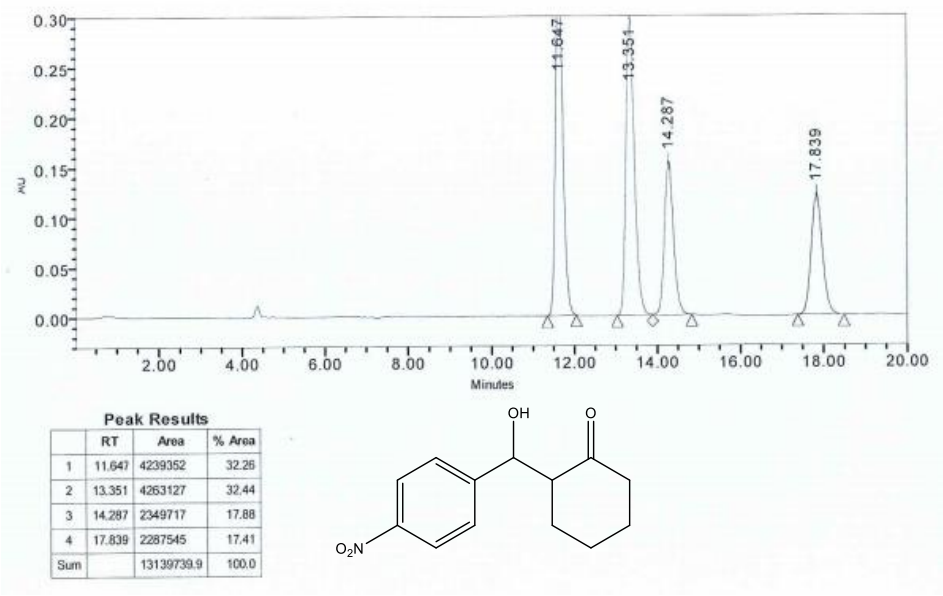


| | RT | Area | % Area |
|---|---|---|---|
| 1 | 11.647 | 4239352 | 32.26 |
| 2 | 13.351 | 4263127 | 32.44 |
| 3 | 14.287 | 2349717 | 17.88 |
| 4 | 17.839 | 2287545 | 17.41 |
| Sum | | 13139739.9 | 100.0 |

**Fig. S36.** HPLC analysis of 2-hydroxy (4-nitrophenyl) methyl) cyclohexan-1-one (Table 1, entry 11).

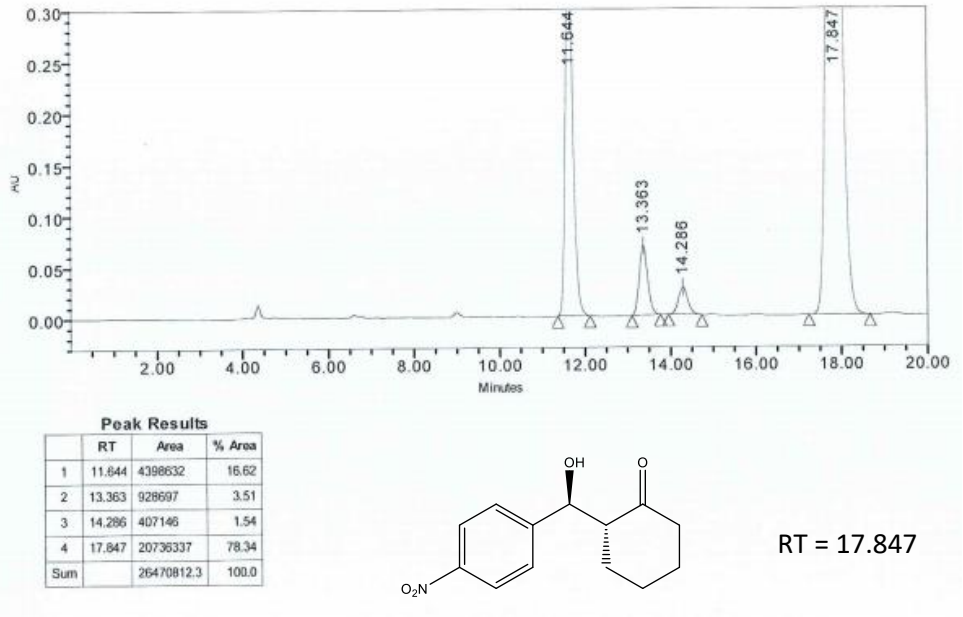


| | RT | Area | % Area |
|---|---|---|---|
| 1 | 11.644 | 4398632 | 16.62 |
| 2 | 13.363 | 928697 | 3.51 |
| 3 | 14.286 | 407146 | 1.54 |
| 4 | 17.847 | 20736337 | 78.34 |
| Sum | | 26470812.3 | 100.0 |

**Fig. S37**. HPLC analysis of (*R*)-2-((*S*)-hydroxy (4-nitrophenyl) methyl) cyclohexan-1-one (Table 1, entry 1).

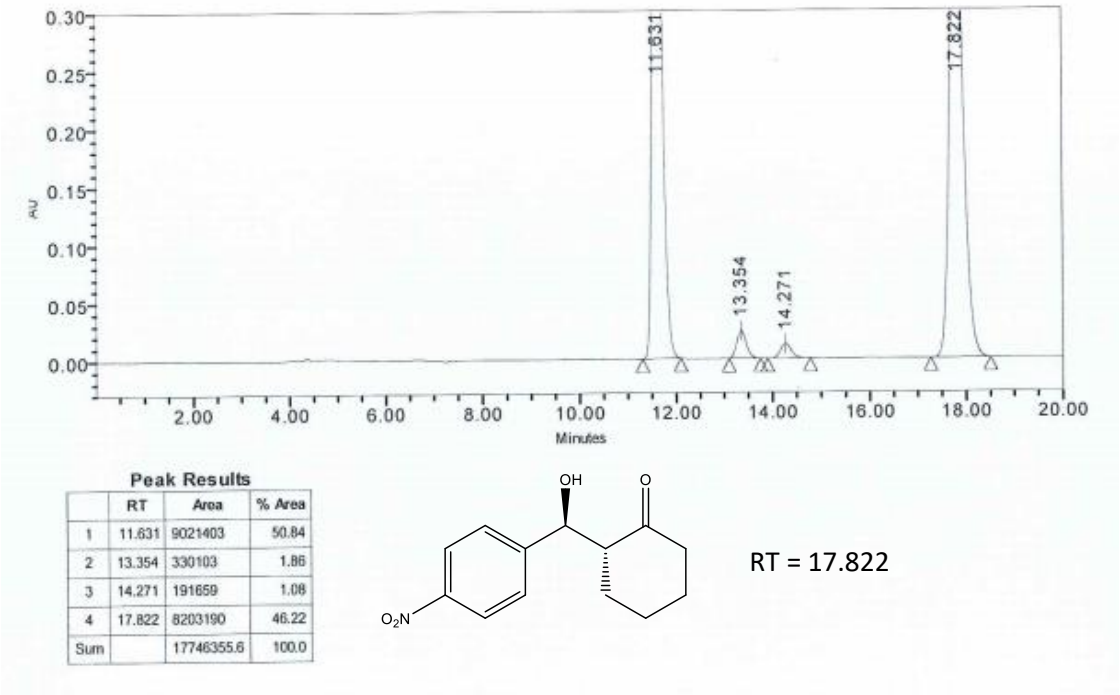


| | RT | Area | % Area |
|---|---|---|---|
| 1 | 11.631 | 9021403 | 50.84 |
| 2 | 13.354 | 330103 | 1.86 |
| 3 | 14.271 | 191659 | 1.08 |
| 4 | 17.822 | 8203190 | 46.22 |
| Sum | | 17746355.6 | 100.0 |

**Fig. S38.** HPLC analysis of (*R*)-2-((*S*)-hydroxy (4-nitrophenyl) methyl) cyclohexan-1-one (Table 1, entry 2).

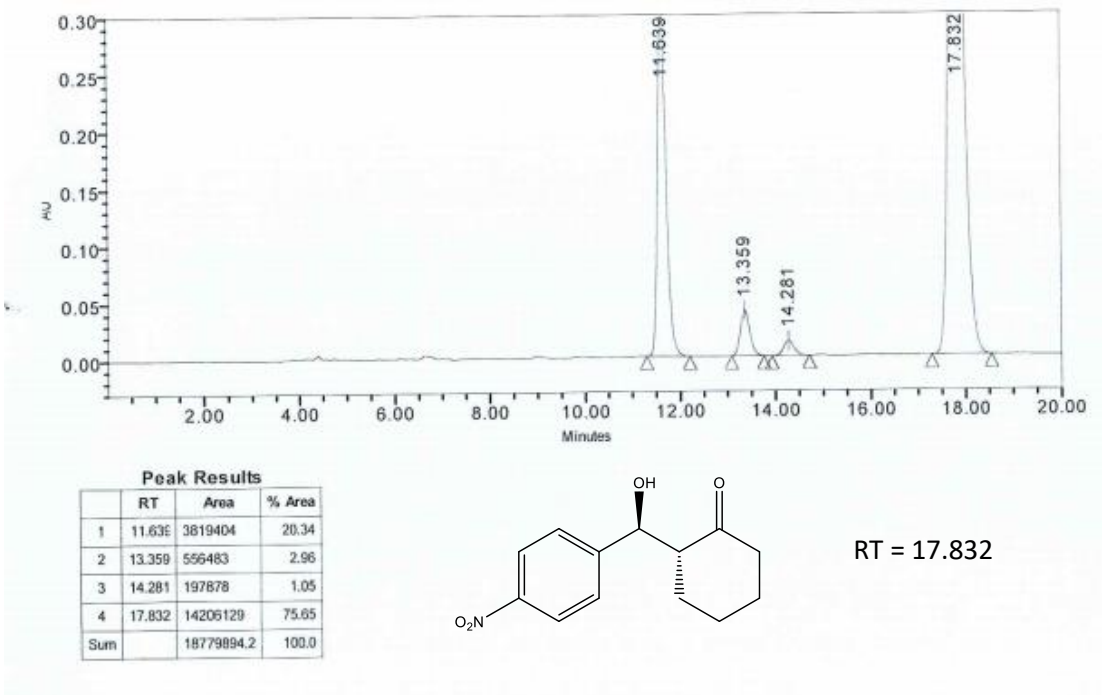


| | RT | Area | % Area |
|---|---|---|---|
| 1 | 11.639 | 3819404 | 20.34 |
| 2 | 13.359 | 556483 | 2.96 |
| 3 | 14.281 | 197878 | 1.05 |
| 4 | 17.832 | 14206129 | 75.65 |
| Sum | | 18779894.2 | 100.0 |

**Fig. S39.** HPLC analysis of (*R*)-2-((*S*)-hydroxy (4-nitrophenyl) methyl) cyclohexan-1-one (Table 1, entry 3).

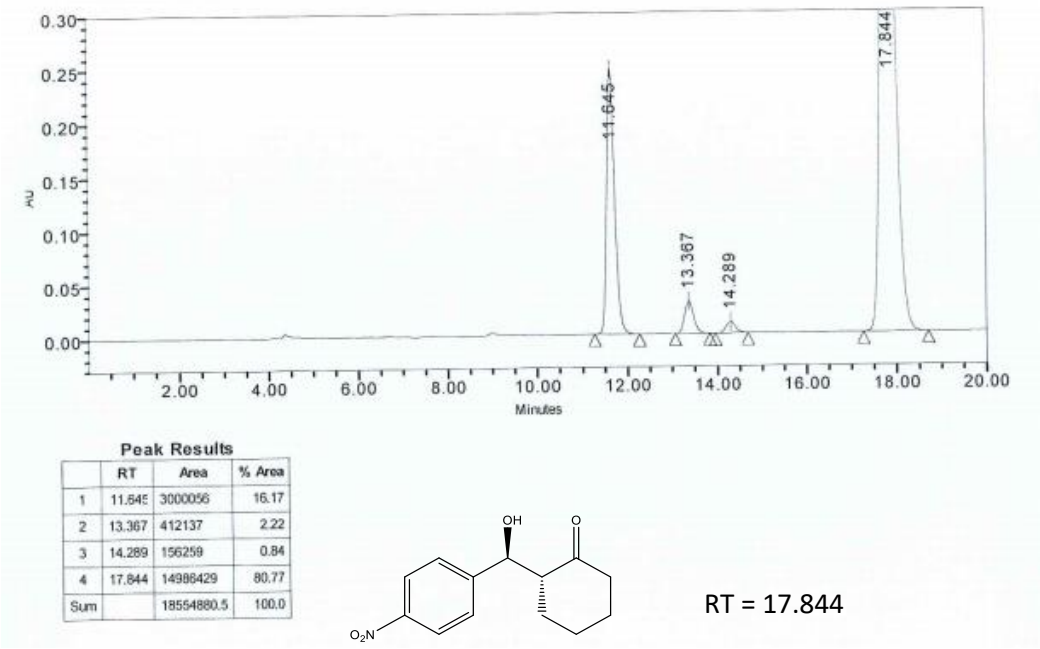


**Fig. S40.** HPLC analysis of (*R*)-2-((*S*)-hydroxy (4-nitrophenyl) methyl) cyclohexan-1-one (Table 1, entry 4).

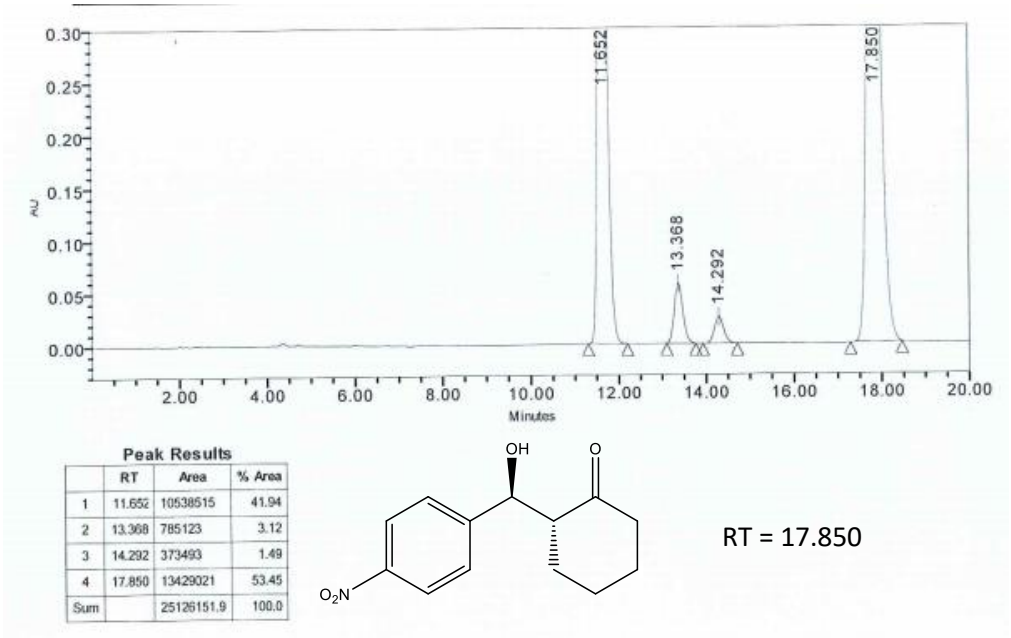


**Fig. S41.** HPLC analysis of (*R*)-2-((*S*)-hydroxy (4-nitrophenyl) methyl) cyclohexan-1-one (Table 2, entry 1).

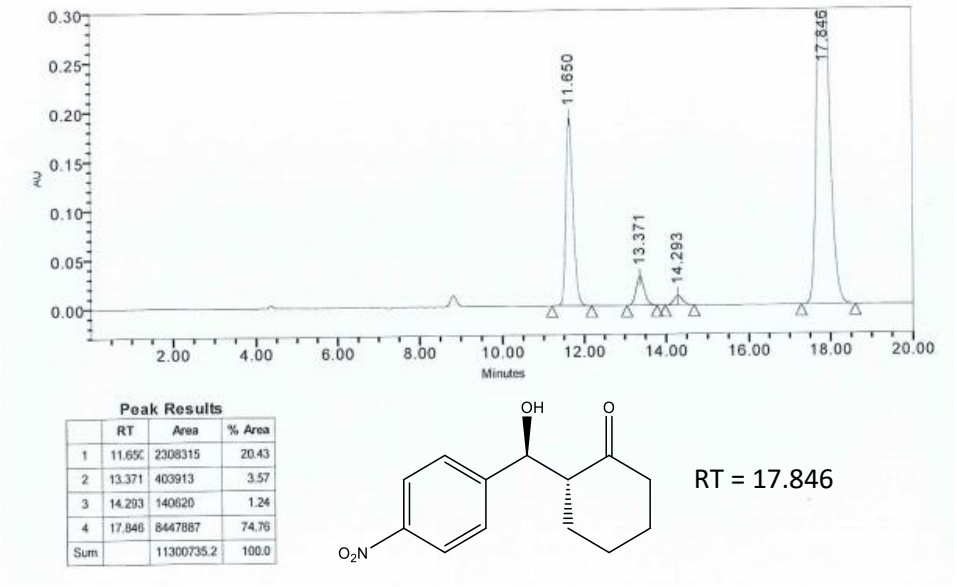


| | RT | Area | % Area |
|---|---|---|---|
| 1 | 11.650 | 2308315 | 20.43 |
| 2 | 13.371 | 403913 | 3.57 |
| 3 | 14.293 | 140620 | 1.24 |
| 4 | 17.846 | 8447887 | 74.76 |
| Sum | | 11300735.2 | 100.0 |

**Fig. S42.** HPLC analysis of (*R*)-2-((*S*)-hydroxy (4-nitrophenyl) methyl) cyclohexan-1-one (Table 2, entry 2).

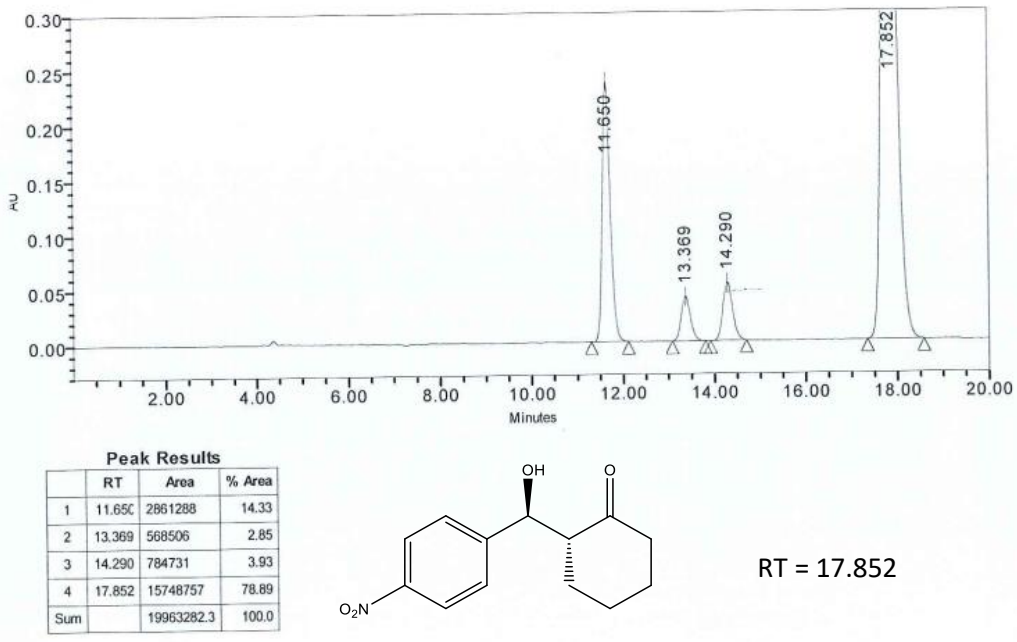


| | RT | Area | % Area |
|---|---|---|---|
| 1 | 11.650 | 2861288 | 14.33 |
| 2 | 13.369 | 568506 | 2.85 |
| 3 | 14.290 | 784731 | 3.93 |
| 4 | 17.852 | 15748757 | 78.89 |
| Sum | | 19963282.3 | 100.0 |

**Fig. S43.** HPLC analysis of (*R*)-2-((*S*)-hydroxy (4-nitrophenyl) methyl) cyclohexan-1-one (Table 2, entry 3).

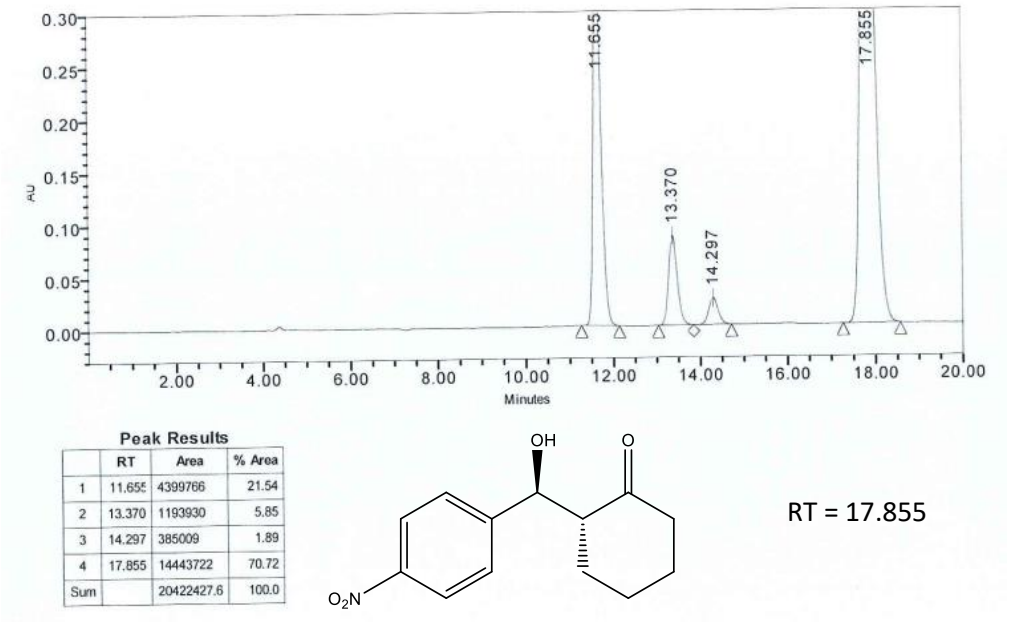


| | RT | Area | % Area |
|---|---|---|---|
| 1 | 11.655 | 4399766 | 21.54 |
| 2 | 13.370 | 1193930 | 5.85 |
| 3 | 14.297 | 385009 | 1.89 |
| 4 | 17.855 | 14443722 | 70.72 |
| Sum | | 20422427.6 | 100.0 |

**Fig. S44.** HPLC analysis of (*R*)-2-((*S*)-hydroxy (4-nitrophenyl) methyl) cyclohexan-1-one (Table 2, entry 4).

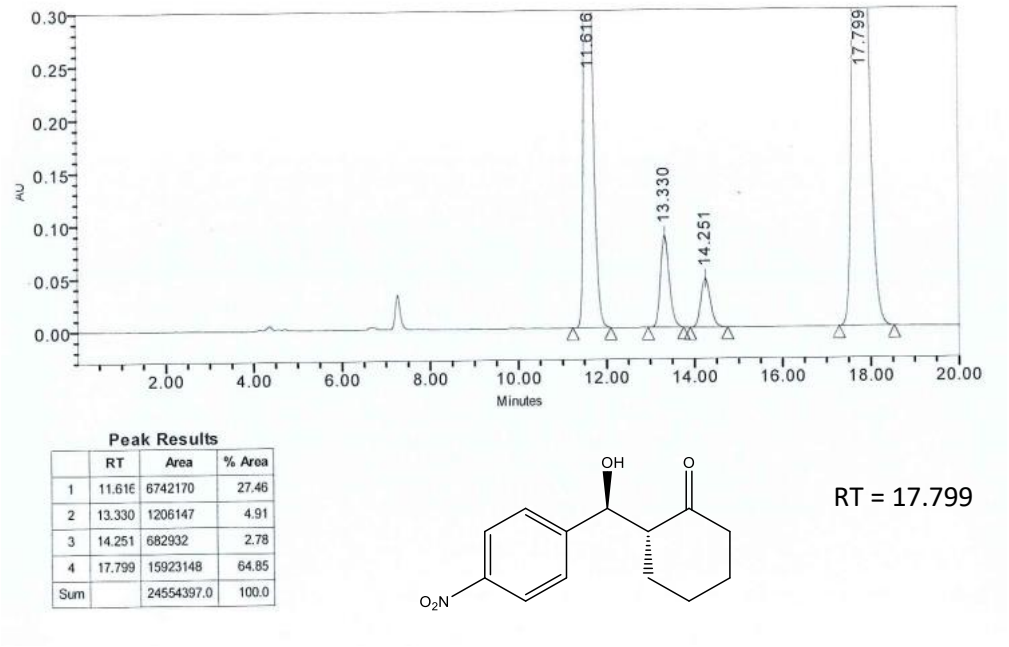


| | RT | Area | % Area |
|---|---|---|---|
| 1 | 11.616 | 6742170 | 27.46 |
| 2 | 13.330 | 1206147 | 4.91 |
| 3 | 14.251 | 682932 | 2.78 |
| 4 | 17.799 | 15923148 | 64.85 |
| Sum | | 24554397.0 | 100.0 |

**Fig. S45.** HPLC analysis of (*R*)-2-((*S*)-hydroxy (4-nitrophenyl) methyl) cyclohexan-1-one (Table 1, entry 7).

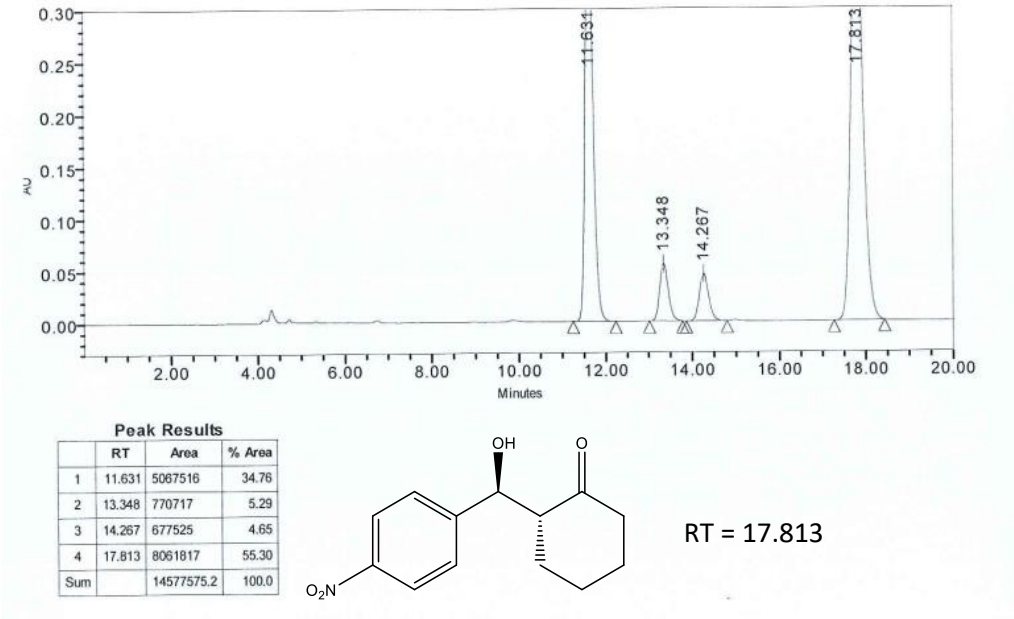


| | RT | Area | % Area |
|---|---|---|---|
| 1 | 11.631 | 5067516 | 34.76 |
| 2 | 13.348 | 770717 | 5.29 |
| 3 | 14.267 | 677525 | 4.65 |
| 4 | 17.813 | 8061817 | 55.30 |
| Sum | | 14577575.2 | 100.0 |

**Fig. S46.** HPLC analysis of (*R*)-2-((*S*)-hydroxy (4-nitrophenyl) methyl) cyclohexan-1-one (Table 1, entry 9).

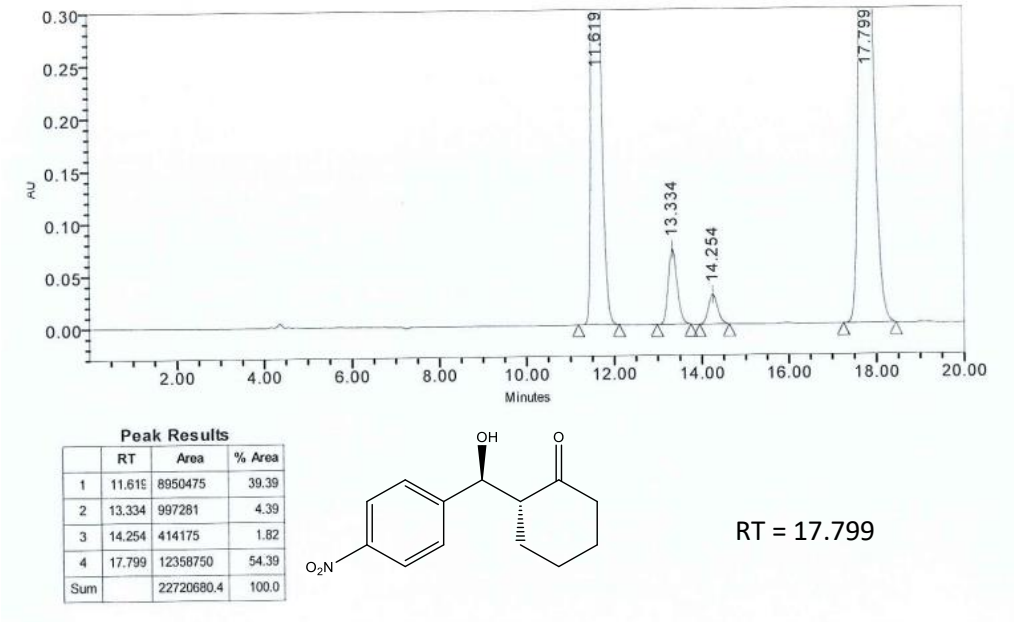


| | RT | Area | % Area |
|---|---|---|---|
| 1 | 11.619 | 8950475 | 39.39 |
| 2 | 13.334 | 997281 | 4.39 |
| 3 | 14.254 | 414175 | 1.82 |
| 4 | 17.799 | 12358750 | 54.39 |
| Sum | | 22720680.4 | 100.0 |

**Fig. S47.** HPLC analysis of (*R*)-2-((*S*)-hydroxyl (4-nitrophenyl) methyl) cyclohexan-1-one (Table 1, entry 10).

### 2.6.7. Computational information

**Table S1.** DFT optimized total energies of the synthesized compounds and transition structures.

| Sr. No. | Compound/State Name | DFT- B3LYP/6-31G Total Energy (Hartree) | | |
|---|---|---|---|---|
| | | | With Cyclohexanone adduct | Transition structures with PNB |
| 1. | (2S,4R)-4-(stearoyloxy)pyrrolidine-2-carboxylic acid **(2)** | -1258.112888 | -1491.578541 | -2041.659070 |
| 2. | (2S,4R)-4-(oleoyloxy)pyrrolidine-2-carboxylic acid **(3)** | -1256.875402 | -1490.341872 | -2040.421857 |
| 3. | (2S,4R)-4-(((9Z,12Z)-octadeca-9,12-dienoyl)oxy)pyrrolidine-2-carboxylic acid **(4)** | -1255.640416 | -1489.104748 | -2039.188410 |
| 4. | (2S,4R)-4-(((9Z,12Z,15Z)-octadeca-9,12,15-trienoyl)oxy)pyrrolidine-2-carboxylic acid **(5)** | -1254.402898 | -1487.868943 | -2037.951724 |
| 5. | Para Nitro Benzaldehyde (PNB) | -550.079066 | - | - |
| 6. | Enamine (chain shorten to one carbon) | -862.514149 | - | - |
| 7. | Reaction **I** (enamine and its complex with PNB) | -1412.595138 | - | - |
| 8. | Reaction **II** (the adduct of reaction between enamine and acetaldehyde) | -1641.708529 | - | - |

## 2.7 References


1. Chen, X.; Zhang, H. -J.; Yang, X.; Lv, H.; Shao, X.; Tao, C.; Wang, H.; Cheng, B.; Li, Y.; Guo, J.; Zhang, J.; Zhai, H. Divergent Total Syntheses of (-)-Daphnilongeranin B and (-)-Daphenylline. *Angew. Chem. Int. Ed.* **2018**, *130*, 959 –963.
2. Heathcock, C. H. *Comprehensive Organic Synthesis*. Trost, B. M.; Fleming, I. Ed.*;* Pergamon Press: Oxford, UK, **1991**; vol. 2, p. 133.
3. Trost, B. M. Atom Economy- A Challenge for Organic Synthesis: Homogeneous Catalysis Leads the Way. *Angew. Chem. Int. Ed.* **1995**, *34*, 259-281.
4. Palomo, C.; Oiarbide, M.; García, J. M. Current Progress in the Asymmetric Aldol Addition Reaction. *Chem. Soc. Rev.* **2004**, *33*, 65 -75.
5. (a) Mukaiyama, T. *Organic Reactions*, John Wiley & Sons Inc: **2004**. (b) Snider, B. B. *Modern Aldol Reactions*, Mahrwald, R., Ed.; Wiley-VCH: Weinheim, Vols. 1 and 2, **2004**.
6. Hajos, Z. G.; Parrish, D. R. *Ger. Pat.* July 29, DE 2102623, **1971**.
7. Hajos, Z. G.; Parrish, D. R. Synthesis and conversion of 2-methyl-2-(3-oxobutyl)-1, 3-cyclopentanedione to the isomeric racemic ketols of the [3.2.1] bicyclooctane and of the perhydroindane series. *J. Org. Chem.* **1974**, *39*, 1615 -1621.
8. Eder, U.; Sauer, G.; Wiechert, R. New Type of Asymmetric Cyclization to Optically Active Steroid CD Partial Structures. *Angew. Chem. Int. Ed. Engl*. **1971**, *10*, 496 -497.
9. List, B.; Lerner, R. A.; Barbas III, C. F. Proline-Catalyzed Direct Asymmetric Aldol Reactions. *J. Am. Chem. Soc.* **2000**, *122*, 2395 -2396.
10. Shah, E.; Soni, H. P. Inducing chirality on ZnS nanoparticles for asymmetric Aldol condensation reactions. *RSC Adv.* **2013**, *3*, 17453 -17461.
11. Mukaiyama, T.; Narasaka, K.; Banno, K. New Aldol Type Reaction. *Chem. Lett.* **1973**, 1011 -1014.
12. Sharma, A. K.; Sunoj, R. B. Enamine versus oxazolidinone: what controls stereoselectivity in proline-catalyzed asymmetric Aldol reactions? *Angew. Chem. Int. Ed.* **2010**, *49*, 6373-6377.
13. Bertelsen, S.; Jørgensen, K. A. Organocatalysis—after the gold rush. *Chem. Soc. Rev.* **2009,** *38*, 2178 -2189.
14. Clayden, J.; Greeves, N.; Warren, S.; Wothers, P. *Organic chemistry*, Oxford University Press: New York, **2001**.

15. Albrecht, Ł.; Jiang, H.; Jørgensen, K. A. Hydrogen-Bonding in Aminocatalysis: From Proline and Beyond. *Chem. Eur. J.* **2014**, *20*, 358-368.
16. Sutar, R. L.; Joshi, N. N. Systematic evaluation of a few proline derivatives as catalysts for a direct Aldol reaction. *Tetrahedron: Asymmetry* **2013**, *24*, 43-49.
17. Vishnumaya, M. R.; Singh, V. K. Highly Efficient Small Organic Molecules for Enantioselective Direct Aldol Reaction in Organic and Aqueous Media. *J. Org. Chem.* **2009**, *74*, 4289-4297.
18. Zotova, N.; Franzke, A.; Armstrong, A.; Blackmond, D. G. Clarification of the Role of Water in Proline-Mediated Aldol Reactions. *J. Am. Chem. Soc.* **2007,** *129*, 15100 –15101.
19. Kristensen, T. E.; Hansen, F. K.; Hansen, T. The Selective O-Acylation of Hydroxyproline as a Convenient Method for the Large-Scale Preparation of Novel Proline Polymers and Amphiphiles. *Eur. J. Org. Chem.* **2009**, 387-395.
20. Kitanosono, T.; Masuda, K.; Xu, P.; Kobayashi, S. Catalytic Organic Reactions in Water toward Sustainable Society. *Chem. Rev.* **2018,** *118*, 679-746.
21. Gijsen, H. J. M.; Qiao, L.; Fitz, W.; Wong, C. -H. Recent Advances in the Chemoenzymatic Synthesis of Carbohydrates and Carbohydrate Mimetics. *Chem. Rev.* **1996,** *96*, 443-474.
22. Blackmond, D. G.; Armstrong, A.; Coombe, V.; Wells, A. Water in organocatalytic processes: debunking the myths. *Angew. Chem. Int. Ed.* **2007,** *46*, 3798-3800.
23. Hayashi, Y. In Water or in the Presence of Water? *Angew. Chem. Int. Ed.* **2006**, *45*, 8103-8104.
24. Mase, N.; Noshiro, N.; Mokuya, A.; Takabe, K. Effect of Long Chain Fatty Acids on Organocatalytic Aqueous Direct Aldol Reactions. *Adv. Synth. Catal.* **2009**, *351*, 2791-2796.
25. Hayashi, Y.; Aratake, S.; Okano, T.; Takahashi, J.; Sumiya, T.; Shoji, M. Combined Proline–Surfactant Organocatalyst for the Highly Diastereo- and Enantioselective Aqueous Direct Cross-Aldol Reaction of Aldehydes. *Angew. Chem. Int. Ed.* **2006**, *45*, 5527-5529.
26. Zhang, S.; Fu, X.; Fu, S. Rationally designed 4-phenoxy substituted prolinamide phenols organocatalyst for the direct Aldol reaction in water. *Tetrahedron Lett.* **2009**, *50*, 1173 - 1176.

27. Zhong, L.; Gao, Q.; Gao, J.; Xiao, J.; Li, C. Direct catalytic asymmetric Aldol reactions on chiral catalysts assembled in the interface of emulsion droplets. *J. Catal.* **2007***, 250,* 360-364.
28. Pera-Titus, M.; Leclercq, L.; Clacens, J. –M.; De Campo, F.; Nardello-Rataj, V. Pickering interfacial catalysis for biphasic systems: from emulsion design to green reactions. *Angew. Chem. Int. Ed.* **2015,** *54,* 2006-2021.
29. Aratake, S.; Itoh, T.; Okano, T.; Nagae, N.; Sumiya, T.; Shoji, M.; Hayashi, Y. Highly Diastereo- and Enantioselective Direct Aldol Reactions of Aldehydes and Ketones Catalyzed by Siloxyproline in the Presence of Water. *Chem. Eur. J.* **2007,** *13,* 10246-10256.
30. Mase, N.; Nakai, Y.; Ohara, N.; Yoda, H.; Takabe, K.; Tanaka, F.; Barbas, C. F., III Highly Diastereo- and Enantioselective Direct Aldol Reactions of Aldehydes and Ketones Catalyzed by Siloxyproline in the Presence of Water. *J. Am. Chem. Soc.* **2006,** *128,* 734-735.
31. Bhadani, A.; Iwabata, K.; Sakai, K.; Koura, S.; Sakaia, H.; Abe, M. Sustainable oleic and stearic acid based biodegradable surfactants. *RSC Adv.* **2017***, 7,* 10433 –10442.
32. Wiesner, M.; Upert, G.; Angelici, G.; Wennemers, H. Enamine Catalysis with Low Catalyst Loadings - High Efficiency via Kinetic Studies. *J. Am. Chem. Soc.* **2010,** *132,* 6-7.
33. Melchiorre, P.; Marigo, M.; Carlone, A.; Bartoli, G. Asymmetric Aminocatalysis—Gold Rush in Organic Chemistry. *Angew. Chem. Int. Ed.* **2008,** *47,* 6138 – 6171.
34. Lombardo, M.; Easwar, S.; Pasi, F.; Trombini, C. The Ion Tag Strategy as a Route to Highly Efficient Organocatalysts for the Direct Asymmetric Aldol Reaction. *Adv. Synth. Catal.* **2009***, 351,* 276 – 282.
35. Zhu, S.; Yu, S.; Ma, D. Highly Efficient Catalytic System for Enantioselective Michael Addition of Aldehydes to Nitroalkenes in Water. *Angew. Chem.* **2008,** *120,* 555-558.
36. Rulli, G.; Duangdee, N.; Baer, K.; Hummel, W.; Berkessel, A.; Gröger, H. Direction of Kinetically versus Thermodynamically Controlled Organocatalysis and Its Application in Chemoenzymatic Synthesis. *Angew. Chem. Int. Ed.* **2011**, *50,* 7944-7947.
37. Vishnumaya, M. R.; Ginotra, S. K.; Singh, V. K. Highly Enantioselective Direct Aldol Reaction Catalyzed by Organic Molecules. *Org. Lett.* **2006,** *8,* 4097 – 4099.

38. Vishnumaya, M. R.; Singh, V. K. Highly Enantioselective Organocatalytic Direct Aldol Reaction in an Aqueous Medium. *Org. Lett.* **2007**, *9*, 2593 – 2595.
39. Vishnumaya, M. R.; Singh, V. K. Organocatalytic reactions in water. *Chem. Commun.* **2009**, 6687-6703.
40. Rankin, K. N.; Gauld, J. W.; Boyd, R. J. Density Functional Study of the Proline-Catalyzed Direct Aldol Reaction. *J. Phys. Chem.* **2002**, *106*, 5155-5159.
41. *Gaussian 09, Revision A.02*, Frisch, M. J.; Trucks, G. W.; Schlegel, H. B.; Scuseria, G. E.; Robb, M. A.; Cheeseman, J. R.; Scalmani, G.; Barone, V.; Mennucci, B.; Petersson, G. A.; Nakatsuji, H.; Caricato, M.; Li, X.; Hratchian, H.P.; Izmaylov, A.F.; Bloino, J.; Zheng, G.; Sonnenberg, J. L.; Hada, M.; Ehara, M.; Toyota, K.; Fukuda, R.; Hasegawa, J.; Ishida, M.; Nakajima, T.; Honda, Y.; Kitao, O.; Nakai, H.; Vreven, T.; Montgomery Jr., J.A.; Peralta, J.E.; Ogliaro, F.; Bearpark, M.; Heyd, J. J.; Brothers, E.; Kudin, K.N.; Staroverov, V.N.; Kobayashi, R.; Normand, J.; Raghavachari, K.; Rendell, A.; Burant, J. C.; Iyengar, S.S.; Tomasi, J.; Cossi, M.; Rega, N.; Millam, J. M.; Klene, M.; Knox, J. E.; Cross, J. B.; Bakken, V.; Adamo, C.; Jaramillo, J.; Gomperts, R.; Stratmann, R.E.; Yazyev, O.; Austin, A.J.; Cammi, R.; Pomelli, C.; Ochterski, J. W.; Martin, R.L.; Morokuma, K.; Zakrzewski, V.G.; Voth, G.A.; Salvador, P.; Dannenberg, J. J.; Dapprich, S.; Daniels, A.D.; Farkas, O.; Foresman, J. B.; Ortiz, J. V.; Cioslowski, J.; Fox, D.J. Gaussian, Inc., Wallingford CT, **2009**.
42. Johnson, E. R.; Keinan, S.; Mori-Sanchez, P.; Contreras-Garcia, J.; Cohen A. J.; Yang, W. T. Revealing Noncovalent Interactions. *J. Am. Chem. Soc.* **2010**, *132*, 6498-6506.